



## Abstract

The radiative forcing estimation of the polluted mineral dust is limited due to lack of morphological analysis, mixing state with the carbonaceous components and the hematite content in the pure dust. The accumulation mode mineral dust has been found to mix with anthropogenically produced black carbon, organic carbon and brown carbon during long range transport. The above features of the polluted dust are not well accounted in the optical models and lead the uncertainty in the numerical estimation of their radiative impact. The Semi-external mixing being a prominent mixing of dust and carbonaceous components has not been studied in details so far compared to core-shell, internal and external mixing studies. In present study, we consider the pure mineral dust composed of non-metallic components (such as Quartz, Feldspar, Mica and Calcite) and metallic component like hematite ( $\text{Fe}_2\text{O}_3$ ). The hematite percentage in the pure mineral dust governs its absorbance. Based on this hematite variation, the hematite fraction in pure mineral dust has been constrained between 0–8%. The morphological and mineralogical characterization of the polluted dust led to consider the three sphere, two sphere and two spheroid model shapes for polluted dust particle system. The pollution gives rise to various light absorbing aerosol components like black carbon, brown carbon and organic carbon (comprising of HUmic-Like Substances, HULIS) in the atmosphere. The entire above discussed model shapes have been considered for the mineral dust getting polluted with (1) organic carbon (especially HULIS component) (2) Brown carbon and (3) black carbon by making a semi-external mixture with pure mineral dust. The optical properties (like Single Scattering Albedo, SSA; Asymmetry parameter,  $g$  and Extinction efficiency,  $Q_{\text{ext}}$ ) of above model shapes for the polluted dust have been computed using Discrete Dipole Approximation, DDA code. For above model shapes, the SSA was found to vary depending on hematite content (0–8%) and model shape composition. For the two sphere BC-mineral dust cluster, hematite was found to be dominating absorber compared to that of black carbon as the  $R_{\text{BC}}/R_{\text{dust}}$  decreases. (i.e. with increase of dust sphere size compared to black carbon

## Effects of particle shape, hematite content and semi-external mixing

S. K. Mishra et al.

Title Page

Abstract

Introduction

Conclusions

References

Tables

Figures

⏪

⏩

◀

▶

Back

Close

Full Screen / Esc

Printer-friendly Version

Interactive Discussion



sphere in the composite 2-sphere cluster). SSA was found to be very sensitivity for the hematite content when both of the spheres (i.e. mineral dust and BC) are nearly of same size. The two spheroid system composed of organic carbon and dust with 0% hematite (OCD'0) showed the maximum deviation of SSA (i.e. ~5%) compared to the two sphere system of same composition and hematite content (OCD-0). Increase in hematite from 0 to 8% caused maximum SSA deviation of ~20% for two sphere organic carbon-dust system (OCD) while the same has been observed to be ~18% for two spheroid organic carbon-dust system (OCD'). SSA was found to be more sensitive to hematite content than that of particle shape. Compared to SSA, Asymmetry parameter,  $g$  was found to be more sensitive towards particle shape. For three-sphere model shapes with 0% hematite composed of black carbon-dust-dust (BCDD-0), brown carbon-dust-dust (BrCDD-0) and organic carbon-dust-dust (OCDD-0), the deviation of SSA and  $g$  relative to conjugate black carbon (BC), brown carbon (BrC) and organic carbon (OC) spheres are ~68% and ~31%, ~83% and ~31% and ~70% and ~33%, respectively. Thus modeled polluted dust optics will provide a better basis for radiative forcing estimation and many sensitivity studies.

## 1 Introduction

The main sources for the mineral dust are the deserts which inject mineral dust in the atmosphere (Goudie et al., 2003; Warren et al., 2007; Schepanski, et al., 2009; Houghton et al., 2001; Xuana et al., 2004; Laurent et al., 2008). Saharan desert itself is solely responsible for half of this amount at global scale. It not only influences the aerosol loading to Africa, the Atlantic Ocean, South America, and the East coast of USA but also to that of Europe. However, the radiative effect of mineral dust is not well quantified (Sokolik and Toon, 1999; Durant et al., 2009; Ginoux et al., 2001; Zender et al., 2003; Kalashnikova et al., 2004; Darmenova et al., 2009; McConnell et al., 2010) and the global radiative forcing due to dust is expected to be negative (Diaz et al., 2001; Myhre et al., 2003; Mahowald and Kiehl, 2003). The mineral dust is transported to long

## Effects of particle shape, hematite content and semi-external mixing

S. K. Mishra et al.

Title Page

Abstract

Introduction

Conclusions

References

Tables

Figures

⏪

⏩

◀

▶

Back

Close

Full Screen / Esc

Printer-friendly Version

Interactive Discussion



distances (Chiapello et al., 1997; Afeti and Resch, 2000; Moulin et al., 1997; Chin et al., 2007; Flaounas et al., 2009) where it gets polluted by mixing with carbonaceous components (forming a polluted dust system) (Jaffe et al., 2003; Maria et al., 2004; Lelieveld et al., 2002). The sources of carbonaceous part are very diverse, which include biomass burning, industrial and vehicular emissions. Thus formed mixture influences the aerosol size distribution, particle shape, hygroscopicity, cloud condensation nuclei and refractive index. The above characteristics of the complex particles govern the optical properties of such particle system whereas the magnitude and sign of the aerosol direct effect is determined by the optical properties of individual aerosols (Lesins et al., 2002).

The radiative effect of dust systems is evaluated by feeding their physical and chemical properties in the radiative models (Tegen et al., 1996; Liao and Seinfeld, 1998; Balkanski et al., 2007; Darmenova et al., 2009; McConnell et al., 2010; Satheesh and Ramanathan, 2000). The sources for the uncertainties in the radiative forcing estimation include mineral aerosol shape (Volten et al., 2005; Zhao et al., 2003; Wang et al., 2003; Kalashnikova and Sokolik, 2002; Mishra et al., 2008), proportion of hematite content in mineral dust (Mishra and Tripathi, 2008) and their mixing states with carbonaceous components (Chandra et al., 2004; Jacobson, 2001). The radiative forcing imposed by the aerosols in the atmosphere can be computed by summing over the entire aerosol population. The assumptions are made on the proportions how the different aerosol components are mixed together. The optical properties of polluted aerosols are numerically estimated with the assumptions that either the particles are mixed externally (where various aerosol species exists independently) (e.g., World Meteorological Organization, 1986; Deepak and Gerbers, 1983; Tegen et al., 1997; Lohmann et al., 1999; Stier et al., 2005; Lesins et al., 2002) or internally mixed (one or several small aerosol particles are imbedded in a larger host particle) (Shinozuka et al., 2009; Ackerman and Toon, 1981; Ch'yalek et al., 1995; Jacobson, 2000; Stier et al., 2006). Core-shell structure of the particle has also been considered in many studies (Moteki et al., 2007; Shiraiwa et al., 2007; Schnaiter et al., 2005; Bond et al., 2006). The real mixed

## Effects of particle shape, hematite content and semi-external mixing

S. K. Mishra et al.

Title Page

Abstract

Introduction

Conclusions

References

Tables

Figures

⏪

⏩

◀

▶

Back

Close

Full Screen / Esc

Printer-friendly Version

Interactive Discussion



## Effects of particle shape, hematite content and semi-external mixing

S. K. Mishra et al.

Title Page

Abstract

Introduction

Conclusions

References

Tables

Figures

⏪

⏩

◀

▶

Back

Close

Full Screen / Esc

Printer-friendly Version

Interactive Discussion



state can be expected to lie somewhere in between the external and internal mixing extremes. The semi-external mixing (two or more aerosol particles are in physical contact and form an aggregate) is such a kind of mixing observed with the individual particle morphological analysis with Scanning Electron Microscopy (SEM), Transmission Electron Microscopy (TEM), High Resolution Transmission Electron Microscopy (HRTEM) and X-ray analysis (Zongbo et al., 2002; Li et al., 2003; Clark et al., 2004; Alexander et al., 2008; Takahama et al., 2010). However, the semi-external mixing is rarely modeled (Mishchenko et al., 2004). As the climatic impact can be estimated based on the radiative forcing estimation so better accounting of the existing mixing state in the optical model will lead to better forcing estimation and hence the better prediction of climatic impacts using General Circulation Model, GCM. In general, the assumption for mixing in GCM is the external mixing (Tegen et al., 1997; Lohmann et al., 1999; Koch et al., 2006; Adams et al., 2001; Shinozuka et al., 2009; Penner et al., 2002; Pierce et al., 2007) which leads to erroneous predictions. Some GCM models also account for internal mixing and core-shell mixing (Menon et al., 2009). Among the carbonaceous components, black carbon (BC), brown carbon (BrC), and the organic carbon (OC) are thought to be major components which mix with the accumulation mode (0.1–1  $\mu\text{m}$  radius) mineral dust during transport over the polluting zone. Among the carbonaceous components, BC is highest absorbing while OC is least and BrC lies in between.

The black carbon particles warrant special attention because of their complex role in climate (Menon et al., 2002; Koch and Genio, 2010; Hill and Dobbie, 2008; Garrett and Zhao, 2006; Ackerman et al., 2000; Penner et al., 1992), long-range transport (Ramamanthan et al., 2001; Rosen et al., 1981; Subramanian et al., 2010), and large surface area that may facilitate heterogeneous reactions (Chughtai et al., 2002). Black carbon (BC) aerosols are different to that of other atmospheric aerosols in terms of their absorbance, heating the air, and contributing to global warming (Hansen et al., 2000; Jacobson, 2001; Menon et al., 2002). Generally the BC aerosols are generated in the atmosphere due to incomplete combustion of fuel oil, coal, and biomass (Ramanathan and Carmichael, 2008; Zhang et al., 2009; Andreae and Merlet, 2001;

Griffin and Goldberg, 1979). The BC particles are generally very hydrophobic but it is converted as hydrophilic because of physical and/or chemical changes occurring during atmospheric aging process (Weingartner et al., 1997; Bauer et al., 2010). The BC aerosols have been well studied in terms of their lifetime, concentration, sources and optical properties on a fixed wavelength (Ogren and Charlson, 1983; Hildemann et al., 1994; Pratsinis, 1994; Hansen et al., 1993; Köhler et al., 2001; Streets et al., 2001). The optical properties of mineral dust externally and internally mixed with BC have been modeled by many scientists (Fuller et al., 1999; Bond and Bergstrom, 2006; Lesins et al., 2002; Jacobson, 2000). Bond et al. (2006) estimated the optical properties of set of combinations of core-shell structure covering the whole range of possible scenarios. In their study, they considered the core to be made of light absorbing carbon while the shell to be of weakly absorbing material. However, detailed research on the optical properties of the mixture of BC with mineral dust (semi-externally mixed) is rarely available. The modeling of optical properties of such externally mixed polluted dust system is very important as has been discussed earlier.

The particles were found to form a semi-external mixtures while the formation of internal mixtures can not be ignored. Liu and Mishchenko (2007) demonstrated the effects of aggregation, fractal morphology, and refractive index on the optical properties of soot aerosols. When the different aerosols form an aggregate (semi-external mixtures) they lie in the near field zone of each other and their scattering and radiative properties can differ from those of composition-equivalent external mixtures. The differences may be too strong that it may influence the results of remote sensing studies of tropospheric aerosols and their radiative forcing estimations (Sato et al., 2003 and references therein) so to reduce the differences, the mineral dust shapes, variation of hematite content ( $\text{Fe}_2\text{O}_3$ ) and the mixing state with all possible carbonaceous components should be accounted together with mineral dust nonsphericity.

To date, there is no rigorous and comprehensive polluted dust optical model available, which deals with the semi-external mixing of mineral dust with all kind of carbonaceous components together with particle nonsphericity and hematite variation (0–8%).

## Effects of particle shape, hematite content and semi-external mixing

S. K. Mishra et al.

Title Page

Abstract

Introduction

Conclusions

References

Tables

Figures

⏪

⏩

◀

▶

Back

Close

Full Screen / Esc

Printer-friendly Version

Interactive Discussion



## Effects of particle shape, hematite content and semi-external mixing

S. K. Mishra et al.

Title Page

Abstract

Introduction

Conclusions

References

Tables

Figures

⏪

⏩

◀

▶

Back

Close

Full Screen / Esc

Printer-friendly Version

Interactive Discussion



In this paper, we consider the pure mineral dust composed of non-metallic components (such as Quartz, Feldspar, Mica and Calcite) and metallic component like hematite ( $\text{Fe}_2\text{O}_3$ ). The deserts are the major sources for the mineral dust and the hematite contribution from these desert dusts found to vary largely (Koven and Fung, 2006). Based on this hematite variation, in this study, the hematite fraction in pure mineral dust has been constrained between 0–8%. The mineralogical composition of pure mineral dust has been considered from the study by Mishra and Tripathi (2008). The morphological and mineralogical characterization of the polluted dust (Shi et al., 2005; Maria et al., 2004; Zongbo et al., 2002; Li et al., 2003; Clark et al., 2004; Alexander et al., 2008; Takhahama et al., 2010) led to consider the three sphere, two sphere and two spheroid model shapes for polluted dust particle system. The pollution gives rise to various light absorbing components like black carbon, brown carbon (Alexander et al., 2008; Andreae and Gelencser, 2006; Yang et al., 2009; Chakrabarty et al., 2010; Moosmüller et al., 2009) and organic carbon comprising of HUmic-Like Substances (HULIS) (Dinar et al., 2008) in the atmosphere. All the above discussed model shapes have been considered for the mineral dust getting polluted with (1) black carbon (2) organic carbon (especially HULIS) and (3) Brown carbon by making Semi-external mixture with pure mineral dust for the hematite range considered in the study. The optical properties like Single Scattering Albedo, SSA, Assymetry parameter,  $g$  and the extinction efficiency,  $Q_{\text{ext}}$  of above model shapes for the polluted dust have been computed using Discrete Dipole Approximation, DDA code (Draine and Flatau, 2004).

## 2 Methodology

The optical properties of the mineral dust semi-externally mixed with the carbonaceous components (BC, BrC and OC) have been modeled for varying hematite (0–8%) and particle nonsphericity. The accumulation mode mineral dust coming from the deserts mixes with the carbonaceous components during long-range transport. The SEM, TEM, HRTEM, and X-ray analysis of various aerosol samples collected from the

atmosphere support the semi-external mixing of the mineral dust with the carbonaceous components (Zongbo et al., 2002; Li et al., 2003; Clark et al., 2004; Alexander et al., 2008; Takahama et al., 2010). Based on the above analysis, the model shapes for the polluted dust systems have been considered and shown in the Fig. 1. Besides the shape, particle size, Aspect Ratio and possibility of existence of considered mixing combinations have been discussed in detail under morphology section (Sect. 3). The consideration of the trace amount of fly ash in some mixing combinations has also been justified in Sect. 3. The optical constants for the components of the polluted dust system have been considered in Sect. 4. The volume equivalent radius, VER of the semi-externally mixed composite dust has been varied from 0.1 to 1.0  $\mu\text{m}$  based on the discussion in Sect. 3. The optical properties of the polluted dust particles described in Fig. 1 have been modeled using DDA (Draine and Flatau, 2004).

### 3 Morphology

The mineral dust particles are not spherical but are characterized by an uneven shape distribution as a function of size. Particle morphology is characterized by the aspect ratio, AR (Reid et al., 2003), a measure of the sphericity of a particle, which is equal to one for a spherical particle and greater than 1 for elongated particles such as ellipsoids.

The mineral dust particles collected in Niger (Nothern Saharan desert) on board the Facility for Airborne Atmospheric Measurements (FAAM) BAe-146 research aircraft, were studied to understand their morphology using a combination of SEM, TEM equipped with an energy dispersive X-ray detection system. The particles have been analyzed using the HISTOLAB program. The AR of about 31 000 sampled particles was studied and found to be practically independent of size for particles of diameter 0.1–10  $\mu\text{m}$ . The upper limit of the AR was found to be 5, whereas the median was 1.7 (Chou et al., 2008). Kandler et al. (2007) reported the AR to be 1.64 for the Saharan Mineral Dust at Izana, Tenerife (Spain), however, Reid et al. (2003) showed a higher value of AR of 1.9 for African mineral dust collected over the Caribbean after being

## Effects of particle shape, hematite content and semi-external mixing

S. K. Mishra et al.

Title Page

Abstract

Introduction

Conclusions

References

Tables

Figures

⏪

⏩

◀

▶

Back

Close

Full Screen / Esc

Printer-friendly Version

Interactive Discussion







there was negligible difference in the optical properties of the composite particle to that of single sphere. So, keeping the above fact in mind, the model shapes have been considered with particles of same size in a cluster. However, the BC-mineral dust two sphere systems have been checked with  $R_{BC}/R_{Dust}$  varying from 0.9 to 1.5 (Fig. 2).  
5 The ratio could not be further reduced due to code limitations.

As the mixing has been found to be significant in the accumulation mode, hence the composite polluted particle radius has been constrained from 0.1–1  $\mu\text{m}$ .

The two-spheroid system comprises of two spheroids of same size attached to each other at  $30^\circ$  orientations. The  $30^\circ$  orientation was more frequent observed feature for the semi-externally mixed spheroids. So, the computations have been performed for  
10 two-spheroid systems with this orientation. Compared to that of two-sphere systems, the probability of getting two-spheroid system has been found to be low.

The three-sphere system comprises three spheres with same size and attached to each other. Takahama et al. (2010) did the rigorous analysis for the particle shape and  
15 distribution of chemical compounds within individual particles using the spectroscopic techniques. In their study, they employed Scanning Transmission X-Ray Microscopy with Near-Edge X-Ray Absorption Fine Structure Spectroscopy with image analysis and pattern recognition techniques to characterize the chemical structure of 636 particles collected on six field campaigns in the western hemisphere between 2004 and  
20 2008. Most of the particles were found to be chemically heterogeneous. Majority of the particles (106) were traced as dust as host with the organic clumps. The majority of the polluted particles lie in the size range between 0.1 and 1  $\mu\text{m}$ .

Based on studies (Takahama et al., 2010; Maria et al., 2004; Moffet et al., 2010), the mineral dust polluted with OC have been considering for different combinations  
25 (spheres with different composition) as 1 OC and 2 dust (OCDD), 2 OC and 1 dust (OCOCD). As the fly-ash is also the major outcome of the combustion processes and the probability of fly-ash to attach the OC-mineral dust cluster can not be ignored so 1 OC + 1 dust + 1 Fly-ash (OCDF) has also been considered as model shape. To the best of our knowledge, there is no literature available till date which could support the

---

## Effects of particle shape, hematite content and semi-external mixing

S. K. Mishra et al.

---

[Title Page](#)[Abstract](#)[Introduction](#)[Conclusions](#)[References](#)[Tables](#)[Figures](#)[⏪](#)[⏩](#)[◀](#)[▶](#)[Back](#)[Close](#)[Full Screen / Esc](#)[Printer-friendly Version](#)[Interactive Discussion](#)

existence of 3-OC cluster (OCOCOC) also OC being the weak absorber; the modeled optical properties for the cluster will not make the major change. Because of these reasons the OCOCOC clusters have not been considered for simulation.

The studies (Alexander et al., 2008; Andreae and Gelencser, 2006; Yang et al., 2009; Chakrabarty et al., 2010; Moosmüller et al., 2009) highlighted the existence of brown carbon in the atmosphere in the spherical form and classified the brown carbon as a special class of OC which is highly absorbing at short wavelengths. Likewise OC, the brown carbon is expected to attach with the mineral dust to form various BrC-mineral dust systems like 1 BrC and 2 dust (BrCDD), 2 BrC and 1 dust (BrCBrCD). The 3-BrC (BrCBrCBrC) system has been modeled to compare with the conjugate BCBCBC system. Because the concept of brown carbon is recently evolved, as our best knowledge no particle image of brown carbon is available to support the 3-BrC model shape. The model shape with 1 BrC + 1 dust + 1 Fly-ash (BrCDF) has not been modeled because of unavailability of the particle images to support the model shape.

Based on electroscopic studies (Zongbo et al., 2002; Liet al., 2003; Clark et al., 2004; Alexander et al., 2008; Moffet et al., 2010) for the mineral dust polluted with BC and fly-ash, various mixing scenarios have been accounted by considering different combinations (spheres with different composition) as 1 BC and 2 dust (BCDD), 2 BC and 1 dust (BCBCD), 1 BC + 1 dust + 1 Fly-ash (BCDF), 3-BC (BCBCBC). The possibility of 3-dust cluster (DDD) is not supported through the chemistry involved in the cluster formation so this system has been ignored. Hereafter, the above combinations will be addressed in abbreviation as given in respective brackets. As the fly-ash has been reported in trace amount in the SEM images so the same has been accounted for the modeling purpose.

Thus using above morphological information and the mixing state, the model shapes have been decided (Fig. 1) for the numerical estimation of the polluted dust optics using DDA model.

## Effects of particle shape, hematite content and semi-external mixing

S. K. Mishra et al.

Title Page

Abstract

Introduction

Conclusions

References

Tables

Figures

⏪

⏩

◀

▶

Back

Close

Full Screen / Esc

Printer-friendly Version

Interactive Discussion



## 4 Polluted dust composition

The polluted dust has been considered to be a semi-external mixture of the pure mineral dust with the carbonaceous components mentioned in Table 2. The optical parameters for the pure mineral dust (composed of Quartz, Feldspar, Mica, Calcite and hematite) at 0.550  $\mu\text{m}$  wavelength have been taken from the study by Mishra and Tripathi (2008) where they varied the hematite percentage to check its effect on the optical properties as hematite is the major absorbing component in the pure mineral dust. The hematite fraction in the global dust has been inferred to be 3.75–11.97% (Koven and Fung, 2006) so to check the sensitivity of the hematite content to the dust optical properties, the optical parameters for 0–8% hematite variation have been considered from Table 1. The optical parameters from Table 1 have been used for modeling the optics of mineral dust mixed with the carbonaceous components while the optical parameters for the carbonaceous components have been taken from Table 2.

A considerable part ( $\sim 10$ – $\rightarrow 50\%$ ) of the atmospheric OC is found to be water-soluble organic carbon (WSOC) (Agarwal et al., 2010; and reference therein; Facchini et al., 1999; Kanakidou et al., 2000). Further, a major fraction ( $> 50\%$ ) of WSOC is composed of high molecular weight multifunctional compounds (Seinfeld, 2006) that contain aromatic, phenolic, and acidic functional groups (Graber and Rudich, 2006; Varga et al., 2001) and called as HUmic-Like Substances (HULIS) because they resemble with Humic Substances (HS) from terrestrial and aquatic sources.

Dinar et al. (2008) measured the refractive indices of the HULIS substance extracted from air pollution particles which were sampled from 18 May 2006 till June 2006 during daytime in an urban location (Weizmann Institute, Rehovot, Israel). The refractive index, ( $m = 1.595 + i0.049$ ) has been measured at 532 nm using a dual-wavelength Cavity Ring Down Aerosol Spectrometer (CRD-AS). The molecular weight ( $M_N$ ) and aromaticity of the HULIS extracted from the pollution particles have been found to be 460 and 16% respectively. This HULIS compound has been considered as the representative of aged organic carbon coming from pollution. In present study, for

### Effects of particle shape, hematite content and semi-external mixing

S. K. Mishra et al.

Title Page

Abstract

Introduction

Conclusions

References

Tables

Figures

⏪

⏩

◀

▶

Back

Close

Full Screen / Esc

Printer-friendly Version

Interactive Discussion

modeling the semi-externally mixed OC-mineral dust clusters, the above mentioned HULIS (i.e. the major fraction of organic carbon) has been considered and represented as OC hereafter.

## 5 Model details

The Optical properties such as SSA, asymmetry parameter,  $g$  and extinction efficiencies,  $Q_{\text{ext}}$  of the polluted dust systems (for the model shapes described in Fig. 1) with the volume equivalent radius,  $\text{VER} < 1 \mu\text{m}$  have been computed using Discrete Dipole Approximation (DDA) (Draine and Flatau, 2004). The DDA model has been used for computing the light scattering of above mentioned polluted dust (semi-externally mixed) accounting for particle nonsphericity. The VER of the non-spherical particle ( $r_{\text{eff}}$ ), refractive index (index of each component in the case of multi components), wavelength ( $\mu\text{m}$ ), particle shape and the particle shape parameters are the inputs to the DDA code. The shape parameters govern the aspect ratio and extent of the target in  $X$ ,  $Y$  and  $Z$  directions whose optical properties are to be modeled. The output of the code is extinction, scattering and absorption efficiencies ( $Q_{\text{ext}}$ ,  $Q_{\text{sca}}$  and  $Q_{\text{abs}}$ ),  $g$ , and the scattering matrix elements.

The DDA model contains routines to generate dipole arrays which represent targets of various geometries like spheres, ellipsoids, rectangular solids, cylinders, hexagonal prisms, tetrahedral, two touching ellipsoids, and three touching ellipsoids. The target has been selected based on our model shapes (Fig. 1). The target dimension is specified in the units of interdipole spacing,  $d$  and the same is fed in the model as the target shape parameters (SHPAR1, SHPAR2, SHPAR3, ...).

The target geometry is described in a coordinate system attached to the target which is referred as “Target Frame” (TF).  $X$ ,  $Y$  and  $Z$  are the coordinates in the Target Frame. For simulating the optical properties of two-sphere and two-spheroid polluted dust systems, the target geometry considered in the DDA model is TWOSPH. This geometry is applicable to two touching homogeneous, isotropic spheroids, with distinct

### Effects of particle shape, hematite content and semi-external mixing

S. K. Mishra et al.

Title Page

Abstract

Introduction

Conclusions

References

Tables

Figures

⏪

⏩

◀

▶

Back

Close

Full Screen / Esc

Printer-friendly Version

Interactive Discussion



compositions. Setting all the dimension same in the geometry helps to generate two sphere particle systems. The parameter, NCOMP shows the number of components in the composite polluted particle. For the above mentioned two sphere and two spheroid dust systems, NCOMP = 2. The optical constant for each spheroid is fed in the model.

5 The BC-mineral dust composite two-sphere system has been modeled for a range of  $R_{BC}/R_{dust}$  values ( $\sim 0.9-1.5$ ) by varying their shape parameters.

For simulating the optical properties of three-sphere polluted dust systems, the target geometry considered in the DDA model is THRELL. This geometry is applicable to three touching homogeneous, isotropic ellipsoids of equal size and orientation, but  
10 distinct compositions. The setting of the entire dimension same for each spheroid in the geometry, helps to generate three sphere particle systems. The parameter, NCOMP shows the number of components in the composite polluted particle. For the three sphere particle system, NCOMP = 3. The optical constant for each spheroid is fed in the model.

## 15 6 Results and discussion

### 6.1 The optical properties of two-particle system

#### 6.1.1 Two-sphere BC-mineral dust system (varying BC and dust particle size in the cluster)

The optical properties of the two-sphere BC-mineral dust system have been modeled for varying sizes of BC and mineral dust. The morphology of such system (Fig. 2) has  
20 already been discussed in Sect. 3.

Figure 3 shows the SSA of the two-sphere BC-mineral dust system for varying effective radius and with hematite variation from 0–8%. The SSA of two sphere BC-dust system has been modeled for decreasing  $R_{BC}/R_{dust}$  (from 1.5 to 0.9) with increasing effective radius (from 0.1 to 0.8  $\mu\text{m}$ ) of the composite particle (Fig. 2). The ratio,  
25  $R_{BC}/R_{dust} = 1$  is for 0.64  $\mu\text{m}$  effective radius of the system.

## Effects of particle shape, hematite content and semi-external mixing

S. K. Mishra et al.

Title Page

Abstract

Introduction

Conclusions

References

Tables

Figures

⏪

⏩

◀

▶

Back

Close

Full Screen / Esc

Printer-friendly Version

Interactive Discussion



## Effects of particle shape, hematite content and semi-external mixing

S. K. Mishra et al.

Title Page

Abstract

Introduction

Conclusions

References

Tables

Figures

⏪

⏩

◀

▶

Back

Close

Full Screen / Esc

Printer-friendly Version

Interactive Discussion



Figure 3 depicts that the two sphere clusters of effective size less than  $0.4\ \mu\text{m}$  are nearly independent of hematite content where  $R_{\text{BC}}/R_{\text{dust}}$  tends to 1.5 with decreasing size. SSA was found to increase with increasing size in this domain. As the  $R_{\text{BC}}/R_{\text{dust}}$  decreases with increasing size (i.e. with increase of dust sphere size compared to black carbon sphere in the composite 2-sphere cluster), hematite starts playing role compared to that of black carbon. The sensitivity of hematite content to SSA is significant when both of the spheres (i.e. mineral dust and BC) in the 2-sphere system, are nearly of same size (Fig. 1). For 2-sphere clusters with effective size greater than  $0.4\ \mu\text{m}$ , the SSA reduces with increasing hematite. In general, SSA was found to increase with size with a maximum in size window  $0.5$  to  $0.6\ \mu\text{m}$  for each hematite content however the maxima is somewhat skewed towards higher sizes for low hematite content.

Figure 4 shows the variation of asymmetry parameter,  $g$  for varying effective size of the particle with hematite varying from 0–8%. Like SSA,  $g$  has also been found to be independent of hematite content for a given size up to effective size less than  $0.4\ \mu\text{m}$ .  $g$  increases with size with a first maximum at  $0.48\ \mu\text{m}$  effective size beyond that it reduces and attains a second maximum at  $0.8\ \mu\text{m}$  size for 8% hematite content. The second maximum is the general feature of particle optics where  $g$  increases with size while the first maxima is due to optimized condition of particle effective size and particle absorbance. For the 2-sphere cluster of  $0.48\ \mu\text{m}$  size, the black carbon sphere is bigger than that of dust sphere and that leads to higher absorbance of the cluster. As the hematite content decreases, the second maximum starts diminishing. For the cluster size greater than  $0.7\ \mu\text{m}$ , the  $g$  was found to increase with increasing hematite content whereas in the size window from  $0.4$  to  $0.7\ \mu\text{m}$ , the variation of  $g$  with hematite content is not significant.

Figure 5 shows the variation of extinction efficiency,  $Q_{\text{ext}}$  for varying effective size of the particle with hematite varying from 0–8%. The  $Q_{\text{ext}}$  increases with size for each hematite content and attains a maxima at  $0.5\ \mu\text{m}$  effective particle size and beyond this size the  $Q_{\text{ext}}$  decreases with size for hematite content less than 4% while vice-versa holds for hematite content  $>4\%$ . The  $Q_{\text{ext}}$  is nearly independent of hematite content for

the effective cluster size less than  $0.22\ \mu\text{m}$ . Beyond this size, the efficiency increases with increasing hematite till  $0.32\ \mu\text{m}$  size. For the size window  $0.32$  to  $0.6\ \mu\text{m}$ , the effect of hematite content on  $Q_{\text{ext}}$  is nearly independent except around  $0.5\ \mu\text{m}$  where it decreases for hematite  $>6\%$ .

For  $0.6$  to  $0.72\ \mu\text{m}$ , where the mineral dust sphere and the black carbon sphere in the 2-sphere cluster, are of nearly of same size, the  $Q_{\text{ext}}$  decreases with increasing hematite while the vice-versa holds good for the size window  $0.75$  to  $0.8\ \mu\text{m}$  where the mineral dust sphere is bigger than that of black carbon sphere for the 2-sphere cluster.

### 6.1.2 Two-sphere (OC-dust and BrC-dust) and two spheroid (OC-dust and BC-dust) particle systems (for same size of the individual particles in the cluster)

Figure 6 shows the SSA of the two-sphere and two spheroid clusters comprising of organic carbon, brown carbon, black carbon and mineral dust with hematite content 0 and 8%. The computations have also been done for the hematite percentage 2, 4 and 6 but have not been shown in Fig. 6. The two sphere OC-dust and BrC-dust systems for 0 and 8% hematite have been represented as OCD-0, BrCD-0 and OCD-8, BrCD-8, respectively. The two spheroid OC-dust and BC-dust systems for 0 and 8% hematite have been represented as OCD'-0, BCD'-0 and OCD'-8, BCD'-8, respectively. The 2-spheroid BrC-dust system could not be considered because of unavailability of particle images which could support the spheroidal morphology of brown carbon. Here, the particles comprising a cluster have been considered of same size. For the comparison purpose, the optical properties of independent homogeneous spheres (of organic carbon (OC), brown carbon (BrC), black carbon (BC) and pure dust sphere with 4% hematite content, D-4) have also been considered. The comparison will be helpful in determining the effect of particle nonsphericity and semi-external mixing of heterogeneous components on the optical properties. Generally, the satellite retrieval algorithms account for the external mixtures of BC and dust homogeneous spheres.

## Effects of particle shape, hematite content and semi-external mixing

S. K. Mishra et al.

Title Page

Abstract

Introduction

Conclusions

References

Tables

Figures

⏪

⏩

◀

▶

Back

Close

Full Screen / Esc

Printer-friendly Version

Interactive Discussion





## Effects of particle shape, hematite content and semi-external mixing

S. K. Mishra et al.

Title Page

Abstract

Introduction

Conclusions

References

Tables

Figures

⏪

⏩

◀

▶

Back

Close

Full Screen / Esc

Printer-friendly Version

Interactive Discussion



The SSA was found to vary depending on hematite content (0 to 8%) for any class of the cluster while different cluster classes showed the variation due to their semi-externally mixed combinations as discussed earlier. For all hematite percentage, the OCD clusters show the higher scattering signature compared to that of BrCD clusters until the effective radius of the cluster reaches to  $0.55\ \mu\text{m}$  and also beyond this threshold size OCD clusters show higher scattering to that of BrCD-8 cluster. The sensitivity of SSA to hematite was found to be insignificant for OCD and OCD' systems compared to that of BrCD and BCD' systems for the effective size  $<0.3\ \mu\text{m}$ . The SSA of the pure dust sphere with 4% hematite content (D-4) showed the highest scattering signature compared to that of any particle cluster. SSA of all the particle clusters have been found in the range which is constrained by that of pure dust (D-4), pure BC and pure BrC spheres. The BC and BrC spheres show nearly same scattering signature for the effective radius  $>0.4\ \mu\text{m}$ . Among all the clusters, the SSA of the semi-externally mixed BrCD-8 cluster significantly differs to that of independent mineral dust, D-4 (~30% SSA variation) for effective particle radius  $>0.5\ \mu\text{m}$  while the same is true for BCD'-0 system for  $<0.3\ \mu\text{m}$ . The BrCD-0 system shows the SSA pattern which could be generated by averaging the SSA of the D-4 and BrC spheres for  $>0.3\ \mu\text{m}$  effective radius. The OCD'-0 spheroid system showed the maximum deviation of SSA (i.e. ~5%) to the OCD-0 sphere system and nearly the same case has been observed for OCD'-8 system relative to that of OCD-8. Increase in hematite from 0 to 8% caused maximum SSA deviation of ~20% for OCD system while the same has been observed to be ~18% for OCD' system. This shows that the SSA is more sensitive to hematite content compared to that of particle shape. BC and BrC spheres show nearly size independent SSA which does not hold good for OC spheres.

Figure 7 shows the asymmetry parameter,  $g$  for the OCD, BrCD, OCD' and BCD' systems for the hematite content 0 and 8%. The  $g$  of OC, BrC, BC and D-4 spheres have also been considered for the reasons discussed earlier. The BrC independent sphere shows the highest asymmetry parameter and tends to the  $g$  value ~0.9 with increasing size. The  $g$  of independent OC and D-4 spheres are more sensitive to the

particle size compared to that of OCD, BrCD, OCD' and BCD' clusters. In general, the  $g$  of the all the clusters and independent spheres have been found to be in the range 0.6 to 0.9. For all the

considered hematite range, the  $g$  of OC-dust clusters (except OCD'-8) have been found to be higher compared to that of independent OC and D-4 spheres for the effective size  $<0.5\ \mu\text{m}$ . This shows that in the above size regime the  $g$  value of semi-externally mixed OC-dust clusters will be underestimated if we consider an external mixture of OC and dust in the aerosol optical model. At  $0.8\ \mu\text{m}$  effective size, the  $g$  values of BrCD-0, BrCD-8, OCD'0, OCD-0, OCD-8, and BCD'-0 systems are over-estimated if we consider an external mixture of OC, BrC, BC and D-4 spheres. At  $1.0\ \mu\text{m}$  effective size, the  $g$  values of OCD-8, BCD'-8, OCD'-8, BrCD-0, BCD'-0 and OCD'-0 systems are well constrained by the  $g$  values of independent OC, BrC, BC and D-4 spheres. The OCD'-8 spheroid system showed the maximum deviation in  $g$  (i.e.  $\sim 11\%$ ) to the OCD-8 sphere system while OCD'-0 system showed the maximum variation (i.e.  $8\%$ ) relative to that of OCD-0. This indicates that compared to SSA,  $g$  is more sensitive towards the particle shape. Increase in hematite from 0 to 8% caused maximum  $g$  deviation of  $\sim 14\%$  for OCD system while the same has been observed to be  $\sim 18\%$  for OCD' system.

Figure 8 shows the extinction efficiency,  $Q_{\text{ext}}$  for the systems discussed in Figs. 6 and 7. No regular pattern of  $Q_{\text{ext}}$  with effective size could be observed for the considered 2-sphere and 2-spheroid clusters. For the effective size window  $0.4\text{--}0.6\ \mu\text{m}$ , the extinction efficiency of the semi-externally mixed OCD, BrCD, OCD' and BCD' clusters have been estimated to be greater than that of OC, BrC, BC and D-4 independent spheres.

## 6.2 The optical properties of three-particle system

The optical properties of the 3-sphere particle system comprising of black carbon (BC), organic carbon (OC), brown carbon (BrC), fly-ash (F) and dust (D) with hematite content  $0\text{--}8\%$  have been modeled. The three spherical particles forming a cluster have been considered of same size in this study.

### Effects of particle shape, hematite content and semi-external mixing

S. K. Mishra et al.

Title Page

Abstract

Introduction

Conclusions

References

Tables

Figures

⏪

⏩

◀

▶

Back

Close

Full Screen / Esc

Printer-friendly Version

Interactive Discussion







found to be reduced with increasing hematite content from 0 to 8.

Till date there are limited experimental observations for the measurement of the asymmetry parameter,  $g$ . The uncertainty involved in the measurement is significant. So the modeling tools play significant role in the numerical estimation of  $g$  by accounting real particle morphology, heterogeneous composition and the mixing states in the optical model.

Among all the accumulation mode dust-carbonaceous species clusters discussed in Fig. 9, the SSA for the BCDD-0 (or BCDF-0) shows the highest deviation  $\sim 68\%$  (relative to BC sphere), for BrCDD-0 cluster  $\sim 83\%$  (relative to BrC sphere) and  $\sim 70\%$  for OCDD-0 (or OCDF-0) cluster (relative to OC sphere). The maximum deviations have been shown for the respective classes in the accumulation mode. These differences may be due to cluster nonsphericity and the cluster heterogeneity.

Figure 10 shows the asymmetry parameter,  $g$  for all the particle systems discussed in Fig. 9. The  $g$  of OC, BrC, BC and D-4 spheres have been modeled for the reasons discussed earlier in Fig. 9. The BrCBrCBrC cluster together with BrC sphere show the highest  $g$  for the accumulation mode polluted dust systems. The BCBCBC cluster together with BC sphere show slightly lesser  $g$  values. First of all, we consider the  $g$  of OC-dust systems. For the effective radius  $< 0.6 \mu\text{m}$ , all the semi-externally mixed OCDF clusters show the energy scattered in the forward direction (i.e.  $g$ ) to be greater than that of OC and D-4 independent spheres while vice versa holds good for size range  $0.73\text{--}0.9 \mu\text{m}$ . Thus neglecting the semi-external mixing and consideration of independent component spheres will lead to underestimation of  $g$  values for the effective radius  $< 0.6 \mu\text{m}$  and the vice versa for radius range  $0.73\text{--}0.9 \mu\text{m}$ . The asymmetry parameters of independent D-4 sphere is most sensitive to the particle size compared to that of OCDF, OCDD and OCOCD semi-externally mixed clusters.

Among the BrC-dust systems, for the effective radius range  $0.72\text{--}0.9 \mu\text{m}$ , the semi-externally mixed BrCDD clusters with the cluster constituents like dust and brown carbon show the energy scattered in the forward direction is smaller than that of energy scattered by BrC and D-4 independent spheres. Thus neglecting the semi-external

## Effects of particle shape, hematite content and semi-external mixing

S. K. Mishra et al.

Title Page

Abstract

Introduction

Conclusions

References

Tables

Figures

⏪

⏩

◀

▶

Back

Close

Full Screen / Esc

Printer-friendly Version

Interactive Discussion



mixing of BrCDD clusters and consideration of independent component spheres will lead to overestimation of  $g$  values for the effective radius range 0.72–0.9  $\mu\text{m}$ .

In case of BC-dust systems, for the effective radius range 0.75–0.9  $\mu\text{m}$ , the semi-externally mixed BCDF and BCDD clusters with the cluster constituents like dust, black carbon and fly-ash show the lesser  $g$  values than that of BC and D-4 independent spheres. This indicates that, for the effective radius range 0.75–0.9  $\mu\text{m}$ , the  $g$  values are overestimated if we replace the semi-external mixing state (presented here in form of 3-sphere clusters) by external mixing of BC and D-4 spheres.

Among all the clusters discussed in Fig. 10, the  $g$  for the BCDD-0 (or BCDF-0) shows the highest deviation  $\sim 31\%$  (relative to BC sphere), for BrCDD-0 cluster  $\sim 31\%$  (relative to BrC sphere) and  $\sim 33\%$  for OCDD-0 (or OCDF-0) cluster (relative to OC sphere).

Figure 11 shows the extinction efficiency,  $Q_{\text{ext}}$  for the carbonaceous species and dust mixture model clusters for which SSA and  $g$  have been shown in Figs. 9 and 10 respectively. As has been observed in Sect. 6.1.2 for the two particle systems, no regular pattern of  $Q_{\text{ext}}$  with effective size could be observed for the considered three sphere particle clusters. The  $Q_{\text{ext}}$  of the semi-externally mixed OC-dust, BrC-dust and BC-dust clusters have been estimated to be greater than that of OC and D-4 (for size window 0.34–0.7  $\mu\text{m}$ ), BrC and D-4 (for the size window 0.38–0.7  $\mu\text{m}$ ) and BC and D-4 independent spheres (for the size window 0.4–0.76  $\mu\text{m}$ ) respectively.

## 7 Conclusions

We modeled the optical properties of several cases of semi-external mixing of carbonaceous components and mineral dust. The main findings can be summarized as follows.

1. The SSA was found to vary depending on hematite content (0–8%) for any class of the cluster while different cluster classes showed the variation due to their

### Effects of particle shape, hematite content and semi-external mixing

S. K. Mishra et al.

Title Page

Abstract

Introduction

Conclusions

References

Tables

Figures

⏪

⏩

◀

▶

Back

Close

Full Screen / Esc

Printer-friendly Version

Interactive Discussion



## Effects of particle shape, hematite content and semi-external mixing

S. K. Mishra et al.

Title Page

Abstract

Introduction

Conclusions

References

Tables

Figures



Back

Close

Full Screen / Esc

Printer-friendly Version

Interactive Discussion



semi-externally mixed heterogeneous combinations. The SSA of the pure dust sphere with 4% hematite content (D-4) showed the highest scattering signature compared to all the clusters considered in the study. The sensitivity of SSA to hematite was found to decrease with reducing number of dust spheres in a particle cluster.

2. The extinction efficiency of the semi-externally mixed clusters was estimated to be greater than that of component species spheres for a size window of 0.3–0.8  $\mu\text{m}$ ,
3. In view of effective absorbance of two sphere BC-mineral dust clusters, hematite starts playing role compared to that of black carbon as the  $R_{\text{BC}}/R_{\text{dust}}$  decreases (i.e. with increase of dust sphere size compared to black carbon sphere in the composite 2-sphere cluster). The sensitivity of SSA to hematite content was found to be significant when both of the spheres (i.e. mineral dust and BC) are nearly of same size.
4. The SSA of the semi-externally mixed BrCD-8 cluster differs most significantly to that of independent mineral dust, D-4 ( $\sim 30\%$  SSA variation) for effective particle radius  $> 0.5 \mu\text{m}$  while the same is true for BCD'-0 system for  $< 0.3 \mu\text{m}$ . The OCD'-0 spheroid system showed the maximum deviation of SSA (i.e.  $\sim 5\%$ ) compared to the OCD-0 and nearly same deviation has been observed for OCD'-8 system relative to that of OCD-8. Increase in hematite from 0 to 8% caused maximum SSA deviation of  $\sim 20\%$  for OCD system while the same has been observed to be  $\sim 18\%$  for OCD' system. This shows that the SSA is more sensitive to hematite content compared to that of particle shape. In general, the  $g$  of the all the clusters and independent spheres have been found to be in the range 0.6 to 0.9. The OCD'-8 spheroid system showed the maximum deviation in  $g$  (i.e.  $\sim 11\%$ ) compared to the OCD-8 sphere system while OCD'-0 system showed the maximum variation (i.e. 8%) relative to that of OCD-0. This indicates that compared to SSA,  $g$  is more sensitive to the particle shape. Increase in hematite from 0 to 8%

caused maximum  $g$  deviation of  $\sim 14\%$  for OCD system while the same has been observed to be  $\sim 18\%$  for OCD' system.

5. The replacement of one dust sphere from OCDD (BrCDD) cluster with one organic carbon (brown carbon) sphere reduces the scattering nature of newly formed OCOCD (BrCBrCD) cluster for the considered hematite contents. Among the accumulation mode dust-carbonaceous species, the SSA for the BCDD-0 (or BCDF-0) shows the highest deviation  $\sim 68\%$  (relative to BC sphere), for BrCDD-0 cluster  $\sim 83\%$  (relative to BrC sphere) and  $\sim 70\%$  for OCDD-0 (or OCDF-0) cluster (relative to OC sphere).
6. The  $g$  value of clusters, like BCDD-0 (or BCDF-0) shows the highest deviation  $\sim 31\%$  (relative to BC sphere), for BrCDD-0 cluster  $\sim 31\%$  (relative to BrC sphere) and  $\sim 3\%$  for OCDD-0 (or OCDF-0) cluster (relative to OC sphere). The differences in SSA and  $g$  may be due to cluster nonsphericity and the cluster heterogeneity.
7. The modeled optical properties of the accumulation mode mineral dust mixed with the carbonaceous species for hematite (0–8%) will be valuable input in the GCM to further reduce the uncertainty in the direct and indirect radiative forcing. Till date no GCM account for the semi-external mixing for the radiative forcing estimation. The database of the optical properties for the mono-disperse particles can be used for the quantified radiative forcing estimation corresponding to different class of clusters accounting particle nonsphericity and heterogeneity. As the semi-external mixing has not been accounted so far in GCM so the modeled optical properties can directly be used for the radiative forcing estimation.

*Acknowledgements.* This research is supported through grants from ISRO MT and GBP and DST ICRP programs.

## Effects of particle shape, hematite content and semi-external mixing

S. K. Mishra et al.

Title Page

Abstract

Introduction

Conclusions

References

Tables

Figures



Back

Close

Full Screen / Esc

Printer-friendly Version

Interactive Discussion





## References

- Ackerman, T. P. and Toon, O. B.: Absorption of visible radiation in atmosphere containing mixtures of absorbing and non-absorbing particles, *Appl. Opt.*, 20, 3661–3668, 1981.
- Ackerman, A. S., Toon, O. B., Stevens, D. E., Heymsfield, A. J., Ramanathan, V., and Welton, E. J.: Reduction of tropical cloudiness by soot, *Science*, 288, 1042–1047, 2000.
- Adams, P. J., Seinfeld, J. H., Koch, D., Mickley, L., and Jacob, D.: General circulation model assessment of direct radiative forcing by the sulfate-nitrate-ammonium-water inorganic aerosol system, *J. Geophys. Res.*, 106, 1097–1111, 2001.
- Afeti, G. M. and Resch, F. J.: Physical characteristics of Saharan dust near the Gulf of Guinea, *Atmos. Environ.*, 34, 1273–1279, 2000.
- Agarwal, S., Aggarwal, S. G., Okuzawa, K., and Kawamura, K.: Size distributions of dicarboxylic acids, ketoacids,  $\alpha$ -dicarbonyls, sugars, WSOC, OC, EC and inorganic ions in atmospheric particles over Northern Japan: implication for long-range transport of Siberian biomass burning and East Asian polluted aerosols, *Atmos. Chem. Phys.*, 10, 5839–5858, doi:10.5194/acp-10-5839-2010, 2010.
- Alexander, D. T. L., Crozier, P. A., Anderson, J. R.: Brown carbon spheres in East Asian outflow and their optical properties, *Science*, 321, 833–836, 2008.
- Andreae, M. O. and Gelencsér, A.: Black carbon or brown carbon? The nature of light-absorbing carbonaceous aerosols, *Atmos. Chem. Phys.*, 6, 3131–3148, doi:10.5194/acp-6-3131-2006, 2006.
- Andreae, M. O. and Merlet, P.: Emissions of trace gases and aerosols from biomass burning, *Global Biogeochem. Cy.*, 15, 955–966, 2001.
- Balkanski, Y., Schulz, M., Claquin, T., and Guibert, S.: Reevaluation of Mineral aerosol radiative forcings suggests a better agreement with satellite and AERONET data, *Atmos. Chem. Phys.*, 7, 81–95, doi:10.5194/acp-7-81-2007, 2007.
- Bauer, S. E., Wright, D. L., Koch, D., Lewis, E. R., McGraw, R., Chang, L.-S., Schwartz, S. E., and Ruedy, R.: MATRIX (Multiconfiguration Aerosol TRacker of mIXing state): an aerosol microphysical module for global atmospheric models, *Atmos. Chem. Phys.*, 8, 6003–6035, doi:10.5194/acp-8-6003-2008, 2008.
- Bauer, S. E., Menon, S., Koch, D., Bond, T. C., and Tsigaridis, K.: A global modeling study on carbonaceous aerosol microphysical characteristics and radiative effects, *Atmos. Chem. Phys.*, 10, 7439–7456, doi:10.5194/acp-10-7439-2010, 2010.

### Effects of particle shape, hematite content and semi-external mixing

S. K. Mishra et al.

Title Page

Abstract

Introduction

Conclusions

References

Tables

Figures

⏪

⏩

◀

▶

Back

Close

Full Screen / Esc

Printer-friendly Version

Interactive Discussion



## Effects of particle shape, hematite content and semi-external mixing

S. K. Mishra et al.

Title Page

Abstract

Introduction

Conclusions

References

Tables

Figures

⏪

⏩

◀

▶

Back

Close

Full Screen / Esc

Printer-friendly Version

Interactive Discussion



- Bond, T. C. and Bergstrom, R. W.: Light absorption by carbonaceous particles: An investigative review, *Aerosol Sci. Technol.*, 40, 27–67, 2006.
- Bond, T. C., Habib, G., and Bergstrom, R. W.: Limitations in the enhancement of visible light absorption due to mixing state, *J. Geophys. Res.*, 111, D20211, doi:10.1029/2006JD007315, 2006.
- 5 Chakrabarty, R. K., Moosmüller, H., Chen, L.-W. A., Lewis, K., Arnott, W. P., Mazzoleni, C., Dubey, M. K., Wold, C. E., Hao, W. M., and Kreidenweis, S. M.: Brown carbon in tar balls from smoldering biomass combustion, *Atmos. Chem. Phys.*, 10, 6363–6370, doi:10.5194/acp-10-6363-2010, 2010.
- 10 Chandra, S., Satheesh, S. K., and Srinivasan, J.: Can the state of mixing of black carbon aerosols explain the mystery of “excess” atmospheric absorption?, *Geophys. Res. Lett.*, 31, L19109, doi:10.1029/2004GL020662, 2004.
- Chiappello, I., Bergametti, G., Chatenet, B., Bousquet, P., Dulac, F., and Santos Soares, E.: Origins of African dust transported over the northeastern tropical Atlantic, *J. Geophys. Res.*, 102, 13 701–13 709, 1997.
- 15 Chin, Mian, Diehl, T., Ginoux, P., and Malm, W.: Intercontinental transport of pollution and dust aerosols: implications for regional air quality, *Atmos. Chem. Phys.*, 7, 5501–5517, doi:10.5194/acp-7-5501-2007, 2007.
- Chou, C., Formenti, P., Maille, M., Ausset, P., Helas, G., Harrison, M., and Osborne, S.: Size distribution, shape, and composition of mineral dust aerosols collected during the African Monsoon Multidisciplinary Analysis Special Observation Period 0: Dust and Biomass-Burning Experiment field campaign in Niger, January 2006, *J. Geophys. Res.*, 113, D00C10, doi:10.1029/2008JD009897, 2008.
- 20 Chughtai, A. R., Kim, J. M., and Smith, D. M.: The effect of air/fuel ration on properties and reactivity of combustion soots, *J. Atmos. Chem.*, 43, 21–43, 2002.
- Ch'yлек, P., Videen, G., Ngo, D., Pinnick, R., and Klett, J.: Effect of black carbon on the optical properties and climate forcing of sulfate aerosols, *J. Geophys. Res.*, 100, 16325–16332, 1995.
- Clarke, A. D., Uehara, T., and Porter, J. N.: Atmospheric nuclei and related aerosol fields over the Atlantic: clean subsiding air and continental pollution during ASTEX, *J. Geophys. Res.*, 102, 25 281–25 292, 1997.
- 30 Clarke, A. D., Shinozuka, Y., Kapustin, V. N., Howell, S., Huebert, B., Doherty, S., Anderson, T., Covert, D., Anderson, J., Hua, X., Moore II, K. G., McNaughton, C., Carmichael,

## Effects of particle shape, hematite content and semi-external mixing

S. K. Mishra et al.

Title Page

Abstract

Introduction

Conclusions

References

Tables

Figures

⏪

⏩

◀

▶

Back

Close

Full Screen / Esc

Printer-friendly Version

Interactive Discussion



G., and Weber, R.: Size distributions and mixtures of dust and black carbon aerosol in Asian outflow: physiochemistry and optical properties, *J. Geophys. Res.*, 109, D15S09, doi:10.1029/2003JD004378, 2004.

5 Darmenova, K., Sokolik, I. N., Shao, Y., Marticorena, B., and Bergametti, G.: Development of a physically based dust emission module within the Weather Research and Forecasting (WRF) model: Assessment of dust emission parameterizations and input parameters for source regions in Central and East Asia, *J. Geophys. Res.*, 114, D14201, doi:10.1029/2008JD011236, 2009.

10 Deepak, A. and Gerbers, H. E.: Report of the experts' meeting on aerosols and their climatic effects, WCP-55 (World Climate Research Program, Geneva), 1983.

Diaz, J. P., Exposito, F. J., Torres, C. J., Herrera, F., Prospero, J. M., and Romero, M. C.: Radiative properties of aerosols in Saharan dust outbreaks using ground-based and satellite data: applications to radiative forcing, *J. Geophys. Res.*, 106, 18403–18416, 2001.

15 Dinar, E., Riziq, A. A., Spindler, C., Erlick, C., Kiss, G., and Rudich, Y.: The complex refractive index of atmospheric and model humic-like substances (HULIS) retrieved by a cavity ring down aerosol spectrometer (CRD-AS), *Faraday Discuss.*, 137, 279–295, 2008.

Draine, B. T. and Flatau, P. J.: User Guide for the Discrete Dipole Approximation Code DDSCAT 6.1, available at: <http://arxiv.org/abs/astro-ph/0409262v2>, 2004.

20 Dubovik, O., Sinyuk, A., Lapyonok, T., Holben, B. N., Mishchenko, M., Yang, P., Eck, T. F., Volten, H., Muñoz, O., Veihelmann, B., van der Zande, W. J., Leon, J.-F., Sorokin, M., and Slutsker, I.: Application of spheroid models to account for aerosol particle nonsphericity in remote sensing of desert dust, *J. Geophys. Res.*, 111, D11208, doi:10.1029/2005JD006619, 2006.

Durant, A. J., Harrison, S. P., Watson, I. M., and Balkanski, Y.: Sensitivity of direct radiative forcing by mineral dust to particle characteristics, *Prog. Phys. Geog.*, 33(1), 80–102, 2009.

25 Fachini, M. C., Fuzzi, S., Zappoli, S., Andracchio, A., Gelencsér, A., Kiss, G., Krivácsy, Z., Mészáros, E., Hansson, H.-C., and Zebühr, Y.: Partitioning of the organic aerosol component between fog droplets and interstitial aerosol, *J. Geophys. Res.*, 104(D21), 26821–26832, doi:10.1029/1999JD900349, 1999.

30 Flaounas, E., Coll, I., Armengaud, A., and Schmechtig, C.: The representation of dust transport and missing urban sources as major issues for the simulation of PM episodes in a Mediterranean area, *Atmos. Chem. Phys.*, 9, 8091–8101, doi:10.5194/acp-9-8091-2009, 2009.

Fuller, K. A., Malm, W. C., and Kreidenweis, S. M.: Effects of Mixing on Extinction By Carbona-

## Effects of particle shape, hematite content and semi-external mixing

S. K. Mishra et al.

Title Page

Abstract

Introduction

Conclusions

References

Tables

Figures

◀

▶

◀

▶

Back

Close

Full Screen / Esc

Printer-friendly Version

Interactive Discussion

ceous Particles, *J. Geophys. Res.*, 104 (D13), 15941–15954, 1999.

Garrett, T. J. and Zhao, C.: Increased Arctic cloud longwave emissivity associated with pollution from mid-latitudes, *Nature*, 440(7085), 787–789, 2006.

5 Ginoux, P., Chin, M., Tegen, I., Prospero, J. M., Holben, B., Dubovik, O., and Lin, S.: Sources and distributions of dust aerosols simulated with the GOCART model, *J. Geophys. Res.*, 106, 20225–20273, 2001.

Goudie, A., Washington, R., Todd, M., and Swann, M.: North African dust production: Source areas and variability, *CLIVAR Exchanges*, 27, 2003.

10 Graber, E. R. and Rudich, Y.: Atmospheric HULIS: How humic-like are they? A comprehensive and critical review, *Atmos. Chem. Phys.*, 6, 729–753, doi:10.5194/acp-6-729-2006, 2006.

Griffin, J. J. and Goldberg, E. D.: Morphologies and origin of elemental carbon in the environment, *Science*, 206, 563–565, 1979.

15 Hansen, A. D. A., Kapustin, V. N., Kopeikin, V. M., Gillette, D. A., and Bodhaine, B. A.: Optical absorption by aerosol black carbon and dust in a desert region of central Asia, *Atmos. Environ.*, 27A(16), 2527–2531, 1993.

Hansen, J., Sato, M., Ruedy, R., Lacis, A., and Oinas, V.: Global warming in the twenty-first century: An alternative scenario, *Proc. Natl. Acad. Sci. USA*, 97, 9875–9880, 2000.

Hess, M., Koepke, P., and Schultz, I.: Optical properties of aerosols and clouds: The software package OPAC, *B. Am. Meteor. Soc.*, 79, 831–844, 1998.

20 Hildemann, L. M., Klinedinst, D. B., Klouda, G. A., Currie, L. A., and Cass, G. R.: Sources of urban contemporary carbon aerosol, *Environ. Sci. Technol.*, 28, 1565–1576, 1994.

Hill, A. A. and Dobbie, S.: The impact of aerosols on nonprecipitating marine stratocumulus. II: The semi-direct effect, *Q. J. Roy. Meteor. Soc.*, 134(634), 1155–1165, doi:10.1002/qj.277, 2008.

25 Jacobson, M. Z.: A physically-based treatment of elemental carbon optics: Implications for global direct forcing of aerosols, *Geophys. Res. Lett.*, 27, 217–220, 2000.

Jacobson, M. Z.: Strong radiative heating due to the mixing state of black carbon in atmospheric aerosols, *Nature*, 409, 695–697, 2001.

Jaffe, D., McKendry, I., Anderson, T., Price, H.: Six “new” episodes of trans-Pacific transport of air pollutants, *Atmos. Environ.*, 37, 391–404, 2003.

30 Kalashnikova, O. V. and Sokolik, I. N.: Importance of shapes and compositions of wind-blown dust particles for remote sensing at solar wavelengths, *Geophys. Res. Lett.*, 29(10), 1398, doi:10.1029/2002GL014947, 2002.

## Effects of particle shape, hematite content and semi-external mixing

S. K. Mishra et al.

Title Page

Abstract

Introduction

Conclusions

References

Tables

Figures

⏪

⏩

◀

▶

Back

Close

Full Screen / Esc

Printer-friendly Version

Interactive Discussion



- Kalashnikova, O. V. and Sokolik, I. N.: Modeling the radiative properties of nonspherical soil-derived mineral aerosols, *J. Quant. Spectrosc. Ra.*, 87, 137–166, 2004.
- Kanakidou, M., Tsigaridis, K., Dentener, F. J., and Crutzen, P. J.: Human-activity-enhanced formation of organic aerosols by biogenic hydrocarbon oxidation, *J. Geophys. Res.*, 105(D7), 9243–9354, doi:10.1029/1999JD901148, 2000.
- Kandler, K., Benker, N., Bundke, U., Cuevas, E., Ebert, M., Knippertz, P., Rodríguez, S., Schütz, L., and Weinbruch, S.: Chemical composition and complex refractive index of Saharan Mineral Dust at Izana, Tenerife (Spain) derived by electron microscopy, *Atmos. Environ.*, 41, 8058–8074, doi:10.1016/j.atmosenv.2007.06.047, 2007.
- Kandler, K., Schütz, L., Deutscher, C., Ebert, M., Hofmann, H., Jäckel, S., Jaenicke, R., Knippertz, P., Lieke, K., Massling, A., Petzold, A., Schladitz, A., Weinzierl, B., Wiedensohler, A., Zorn, S., and Weinbruch, S.: Size distribution, mass concentration, chemical and mineralogical composition, and derived optical parameters of the boundary layer aerosol at Tinfou, Morocco, during SAMUM, 2006, *Tellus*, 61B, 32–50, 2009.
- Koch, D. and Del Genio, A. D.: Black carbon semi-direct effects on cloud cover: review and synthesis, *Atmos. Chem. Phys.*, 10, 7685–7696, doi:10.5194/acp-10-7685-2010, 2010.
- Koch, D., Schmidt, G. A., and Field, C. V.: Sulfur, sea salt and radionuclide aerosols in GISS ModelE, *J. Geophys. Res.*, 111, D06206, doi:10.1029/2004JD005550, 2006.
- Köhler, I., Dameris, M., Ackermann, I., and Hass, H.: Contribution of road traffic emissions to the atmospheric black carbon burden in the mid-1990s, *J. Geophys. Res.*, 106, 17997–18014, 2001.
- Kotzick, R. and Niessner, R.: The effects of the aging process on critical supersaturation ratios of ultrafine carbon aerosols, *Atmos. Environ.*, 33, 2669–2677, 1999.
- Koven, C. D. and Fung, I.: Inferring dust composition from wavelength-dependent absorption in Aerosol Robotic Network (AERONET) data, *J. Geophys. Res.*, 111, D14205, doi:10.1029/2005JD006678, 2006.
- Laurent, B., Marticorena, B., Bergametti, G., Léon, J. F., and Mahowald, N. M.: Modeling mineral dust emissions from the Sahara desert using new surface properties and soil database, *J. Geophys. Res.*, 113, D14218, doi:10.1029/2007JD009484, 2008.
- Lelieveld, J., Berresheim, H., Borrmann, S., Crutzen, P. J., Dentener, F. J., Fischer, H., Feichter, J., Flatau, P. J., Heland, J., Holzinger, R., Korrmann, R., Lawrence, M. G., Levin, Z., Markowicz, K. M., Mihalopoulos, N., Minikin, A., Ramanathan, V., Reus, M. de, Roelofs, G. J., Scheeren, H. A., Sciare, J., Schlager, H., Schultz, M., Siegmund, P., Steil, B., Stephanou,

## Effects of particle shape, hematite content and semi-external mixing

S. K. Mishra et al.

Title Page

Abstract

Introduction

Conclusions

References

Tables

Figures

⏪

⏩

◀

▶

Back

Close

Full Screen / Esc

Printer-friendly Version

Interactive Discussion



E. G., Stier, P., Traub, M., Warneke, C., Williams, J., and Ziereis, H.: Global air pollution crossroads over the Mediterranean, *Science*, 298, 794–799, 2002.

Lesins, G., Chylek, P., and Lohmann, U.: A study of internal and external mixing scenarios and its effect on aerosol optical properties and direct radiative forcing, *J. Geophys. Res.*, 107(D10), doi:10.1029/2001JD000973, 2002.

Liu, F. and Swithenbank, J.: The effects of particle size distribution and refractive index on fly ash radiative properties using a simplified approach, *Int. J. Heat Mass Tran.*, 36, 1905–1912, 1996.

Liu, Li. and Mishchenko, M. I.: Scattering and radiative properties of complex soot and soot-containing aggregate particles, *J. Quant. Spectrosc. Ra.*, 106, 262–273, 2007.

Li, J., Anderson, J. R., and Buseck, P. R.: TEM study of aerosol particles from clean and polluted marine boundary layers over the North Atlantic, *J. Geophys. Res.*, 108(D6), 4189, doi:10.1029/2002JD002106, 2003.

Liao, H. and Seinfeld, J. H.: Radiative forcing by mineral dust aerosols: Sensitivity to key variables, *J. Geophys. Res.*, 103(D24), 31637–31645, 1998.

Lohmann, U., Feichter, J., Chuang, C. C., and Penner, J. E.: Prediction of the number of cloud droplets in the ECHAM GCM, *J. Geophys. Res.*, 104, 9169–9198, 1999.

McConnell, C. L., Formenti, P., Highwood, E. J., and Harrison, M. A. J.: Using aircraft measurements to determine the refractive index of Saharan dust during the DODO Experiments, *Atmos. Chem. Phys.*, 10, 3081–3098, doi:10.5194/acp-10-3081-2010, 2010.

Mahowald, N. and Kiehl, L.: Mineral aerosol and cloud interactions, *Geophys. Res. Lett.*, 30, 1475, doi:10.1029/2002GL016762, 2003.

Maria, S. F., Russel, L. M., Gilles, M. K., and Myneni, S. C. B.: Organic aerosol growth mechanisms and their climate-forcing implications, *Science*, 306, 1921–1924, 2004.

Menon, S., Hansen, J., Nazarenko, L., and Luo, Y.: Climate effects of black carbon aerosols in China and India, *Science*, 297, 2250–2253, 2002.

Menon S., Bauer, S. E., Sednev, I., Koch, D., Morrison, H., and DeMott, P.: Aerosol-climate interactions: Evaluation of cloud processes and regional climate impacts from varying GHG and aerosol amounts, *Atmos. Chem. Phys. Discuss.*, submitted, 2009.

Mishchenko, M. I., Liu, Li, Travis, L. D., Lasis, A. A.: Scattering and radiative properties of semi-external versus external mixtures of different aerosol types, *J. Quant. Spectrosc. Ra.*, 88, 139–147, 2004.

Mishra, S. K. and Tripathi, S. N.: Modeling optical properties of mineral dust over the Indian

## Effects of particle shape, hematite content and semi-external mixing

S. K. Mishra et al.

[Title Page](#)

[Abstract](#)

[Introduction](#)

[Conclusions](#)

[References](#)

[Tables](#)

[Figures](#)

[⏪](#)

[⏩](#)

[◀](#)

[▶](#)

[Back](#)

[Close](#)

[Full Screen / Esc](#)

[Printer-friendly Version](#)

[Interactive Discussion](#)



Desert, J. Geophys. Res., 113, D23201, doi:10.1029/2008JD010048, 2008.

Moffet, R. C., Henn, T. R., Tivanski, A. V., Hopkins, R. J., Desyaterik, Y., Kilcoyne, A. L. D., Tyliczszak, T., Fast, J., Barnard, J., Shutthanandan, V., Cliff, S. S., Perry, K. D., Laskin, A., and Gilles, M. K.: Microscopic characterization of carbonaceous aerosol particle aging in the outflow from Mexico City, Atmos. Chem. Phys., 10, 961–976, doi:10.5194/acp-10-961-2010, 2010.

Moosmüller, H., Chakrabarty, R. K., and Arnott, W. P.: Aerosol light absorption and its measurement: A review, J. Quant. Spectrosc. Ra., 110, 844–878, 2009.

Moteki, N., Kondo, Y., Miyazaki, Y., Takegawa, N., Komazaki, Y., Kurata, G., Shirai, T., Blake, D. R., Miyakawa, T., and Koike, M.: Evolution of mixing state of black carbon particles: Aircraft measurements over the western Pacific in March 2004, Geophys. Res. Lett., 34, L11803, doi:10.1029/2006GL028943, 2007.

Moulin, C., Lambert, C. E., Dulac, F., and Dayan, U.: Control of atmospheric export from North Africa by the North Atlantic Oscillation, Nature, 397, 691–694, doi:10.1038/42679, 1997.

Myhre, G., Grini, A., Haywood, J. M., Stordal, F., Chatenet, B., Tanre, D., Sundet, J. K., and Isaksen, I. S. A.: Modeling the radiative impact of mineral dust during the Saharan Dust Experiment (SHADE) campaign, J. Geophys. Res., 108, 8579, doi:10.1029/2002JD002566, 2003.

Ogren, J. A. and Charlson, R. J.: Elemental carbon in the atmosphere: Cycle and lifetime, Tellus, 35B, 241–254, 1983.

Okada, K., Heintzenberg, J., Kai, K., and Qin, Y.: Shape of atmospheric mineral particles collected in three Chinese arid-regions, Geophys. Res. Lett., 28, 3123–3126, 2001.

Parungo, F., Kim, Y., Zhu, C., Harris, J., Schnell, R., Li, X., Yang, D., Fang, X., Zhou, M., Chen, Z., and Park, K.: Asian Dust storms and their effects on radiation and climate: Part 4, Science and Technology Corporation Technical Report for NOAA, 1997.

Penner, J. E., Dickinson, R. E., and O'Neill, C. A: Effects of aerosol from biomass burning on the global radiation budget, Science, 256, 1432–1434, 1992.

Penner, J. E., Zhang, S. Y., Chin, M., Chuang, C. C., Feichter, J., Feng, Y., Geogdzhayev, I. V., Ginoux, P., Herzog, M., Higurashi, A., Koch, D., Land, C., Lohmann, U., Mishchenko, M., Nakajima, T., Pitari, G., Soden, B., Tegen, I., and Stowe, L.: A comparison of model- and satellitederived aerosol optical depth and reflectivity, J. Atmos. Sci., 59, 441–460, 2002.

Pierce, J. R., Chen, K., and Adams, P. J.: Contribution of primary carbonaceous aerosol to cloud condensation nuclei: processes and uncertainties evaluated with a global aerosol

## Effects of particle shape, hematite content and semi-external mixing

S. K. Mishra et al.

Title Page

Abstract

Introduction

Conclusions

References

Tables

Figures

◀

▶

◀

▶

Back

Close

Full Screen / Esc

Printer-friendly Version

Interactive Discussion

microphysics model, *Atmos. Chem. Phys.*, 7, 5447–5466, doi:10.5194/acp-7-5447-2007, 2007.

Pratsinis, S. E.: Motor vehicle contributions to fine carbonaceous aerosol in Los Angeles, *Aerosol Sci. Technol.*, 21, 360–366, 1994.

5 Ramanathan, V., Crutzen, P. J., Lelieveld, J., Mitra, A. P., Althausen, D., Anderson, J., Andreae, M. O., Cantrell, W., Cass, G. R., Chung, C. E., Clarke, A. D., Coakley, J. A., Collins, W. D., Conant, W. C., Dulac, F., Heintzenberg, J., Heymsfield, A. J., Holben, B., Howell, S., Hudson, J., Jayaraman, A., Kiehl, J. T., Krishnamurti, T. N., Lubin, D., McFarquhar, G., Novakov, T., Ogren, J. A., Podgorny, I. A., Prather, K., Priestley, K., Prospero, J. M., Quinn, P. K.,  
10 Rajeev, K., Rasch, P., Rupert, S., Sadourny, R., Satheesh, S. K., Shaw, G. E., Sheridan, P., and Valero, F. P. J.: Indian Ocean Experiment: An integrated analysis of the climate forcing and effects of the great Indo-Asian haze, *J. Geophys. Res.*, 106(D22), 28371–28398, 2001.

Ramanathan, V. and Carmichael, G.: Global and regional climate changes due to black carbon, *Nature*, 221–227, doi:10.1038/ngeo156, 2008.

15 Reid, E. A., Reid, J. S., Meier, M. M., Dunlap, M. R., Cliff, S. S., Broumas, A., Perry, K., and Maring, H.: Characterization of African dust transported to Puerto Rico by individual particle and size segregated bulk analysis, *J. Geophys. Res.*, 108(D19), 8591, doi:10.1029/2002JD002935, 2003.

Rosen, H., Novakov, T., and Bodhaine, B. A.: Soot in the Arctic, *Atmos. Environ.*, 15, 1371–1374, 1981.

20 Saathoff, H., Naumann, K. H., Schnaiter, M., Schock, W., Mohler, O., Schurath, U., Weingartner, E., Bysel, M., and Baltensperger, U.: Coating of soot and  $(\text{NH}_4)_2\text{SO}_4$  particles by ozonolysis products of -pinene, *J. Aerosol Sci.*, 34, 1297–1321, 2003.

Satheesh, S. K. and Ramanathan, V.: Large differences in the tropical aerosol forcing at the top of the atmosphere and Earth's surface, *Nature*, 405, 60–63, 2000.

25 Sato, M., Hansen, J., Koch, D., Lacis, A., Ruedy, R., Dubovik, O., Holben, B., Chin, M., and Novakov, T.: Global atmospheric black carbon inferred from AERONET., *P. Natl. Acad. Sci.*, 100, 6319–6324, doi:10.1073/pnas.0731897100, 2003.

Schepanski, K., Tegen, I., Todd, M. C., Heinold, B., Boenisch, G., Laurent, B., and Macke, A.: Meteorological processes forcing Saharan dust emission inferred from MSG-SEVIRI observations of subdaily dust source activation and numerical models, *J. Geophys. Res.*, 114, D10201, doi:10.1029/2008JD010325, 2009.

30 Schnaiter, M., Horvath, H., Möhler, O., Naumann, K. H., Saathoff, H., and Schöck, O. W.: UV-



## Effects of particle shape, hematite content and semi-external mixing

S. K. Mishra et al.

Title Page

Abstract

Introduction

Conclusions

References

Tables

Figures

⏪

⏩

◀

▶

Back

Close

Full Screen / Esc

Printer-friendly Version

Interactive Discussion



VIS-NIR spectral optical properties of soot and soot-containing aerosols, *J. Aerosol Sci.*, 34, 1421–1444, 2003.

Schnaiter, M., C., Linke, O., Möler, K. H., Naumann, H., Saathoff, R., Wagner, U., Schurath, and Wehner, B.: Absorption amplification of black carbon internally mixed with secondary organic aerosol, *J. Geophys. Res.*, 110, D19204, doi:10.1029/2005JD006046, 2005.

Schwarz, J. P., Spackman, J. R., Fahey, D. W., Gao, R. S., Lohmann, U., Stier, P., Watts, L. A., Thomson, D. S., Lack, D. A., Pfister, L., Mahoney, M. J., Baumgardner, D., Wilson, J. C., and Reeves, J. M.: Coatings and their enhancement of black carbon light absorption in the tropical atmosphere, *J. Geophys. Res.*, 113, D03203, doi:10.1029/2007JD009042, 2008.

Seinfeld, J. H.: Final Technical Report: DE-FG03-01ER63099/DE-FG02-01ER63099, 1 March 2001–28 February 2005, Department of Energy, California Institute of Technology, Pasadena, CA 91125, available at: <http://www.osti.gov/bridge/purl.cover.jsp;jsessionid=33DCDA9DAA0E871AE143EF9AB0CEFB3F?puhl=/877386-rVUGqH/>, 2006.

Shi, Z. B., Shao, L. Y., Jones, T. P., Whittaker, A. G., Lv, S. L., Bérub'e, K. A., He, T., and Richards, R. J.: Characterization of airborne individual particles collected in an urban area, a satellite city and a clean air area in Beijing, *Atmos. Environ.*, 37(29), 4097–4108, 2003.

Shi, Z., Shao, L., and Jones, T. P., and Lu, S.: Microscopy and mineralogy of airborne particles collected during severe dust storm episodes in Beijing, China, *J. Geophys. Res.*, 110, D01303, doi:10.1029/2004JD005073, 2005.

Shinozuka, Y., Clarke, A. D., DeCarlo, P. F., Jimenez, J. L., Dunlea, E. J., Roberts, G. C., Tomlinson, J. M., Collins, D. R., Howell, S. G., Kapustin, V. N., McNaughton, C. S., and Zhou, J.: Aerosol optical properties relevant to regional remote sensing of CCN activity and links to their organic mass fraction: airborne observations over Central Mexico and the US West Coast during MILAGRO/INTEX-B, *Atmos. Chem. Phys.*, 9, 6727–6742, doi:10.5194/acp-9-6727-2009, 2009.

Shiraiwa, M., Kondo, Y., Moteki, N., Takegawa, N., Miyazaki, Y., and Blake, D. R.: Evolution of mixing state of black carbon in polluted air from Tokyo, *Geophys. Res. Lett.*, 34, L16803, doi:10.1029/2007GL029819, 2007.

Stier, P., Feichter, J., Kinne, S., Kloster, S., Vignati, E., Wilson, J., Ganzeveld, L., Tegen, I., Werner, M., Balkanski, Y., Schulz, M., Boucher, O., Minikin, A., and Petzold, A.: The aerosol-climate model ECHAM5-HAM, *Atmos. Chem. Phys.*, 5, 1125–1156, doi:10.5194/acp-5-1125-2005, 2005.

Stier, P., Seinfeld, J. H., Kinne, S., Feichter, J., and Boucher, O.: Impact of nonabsorbing an-

## Effects of particle shape, hematite content and semi-external mixing

S. K. Mishra et al.

Title Page

Abstract

Introduction

Conclusions

References

Tables

Figures

⏪

⏩

◀

▶

Back

Close

Full Screen / Esc

Printer-friendly Version

Interactive Discussion

thropogenic aerosols on clearsky atmospheric absorption, *J. Geophys. Res.*, 111, D18201, doi:10.1029/2006JD007147, 2006.

Streets, D. G., Gupta, S., Waldhoff, S. T., Wang, M. Q., Bond, T. C., and Bo, Y.: Black carbon emissions in China, *Atmos. Environ.*, 35, 4281–4296, 2001.

5 Subramanian, R., Kok, G. L., Baumgardner, D., Clarke, A., Shinozuka, Y., Campos, T. L., Heizer, C. G., Stephens, B. B., de Foy, B., Voss, P. B., and Zaveri, R. A.: Black carbon over Mexico: the effect of atmospheric transport on mixing state, mass absorption cross-section, and BC/CO ratios, *Atmos. Chem. Phys.*, 10, 219–237, doi:10.5194/acp-10-219-2010, 2010.

10 Takahama, S., Liu, S., and Russell, L. M.: Coatings and clusters of carboxylic acids in carbon-containing atmospheric particles from spectromicroscopy and their implications for cloud-nucleating and optical properties, *J. Geophys. Res.*, 115, D01202, doi:10.1029/2009JD012622, 2010.

Tegen, I., Lacis, A. A., and Fung, I.: The influence on climate forcing of mineral aerosols from disturbed soils, *Nature*, 380, 419–421, doi:10.1038/38041900, 1996.

15 Tegen, I., Hollrig, P., Chin, M., Fung, I., Jacob, D., and Penner, J.: Contribution of different aerosol species to the global aerosol extinction optical thickness: Estimates from model results, *J. Geophys. Res.*, 102, 23895–23916, 1997.

Varga, B., Kiss, G., Ganszky, I., Gelencsér, A., and Krivácsy, Z.: Isolation of water-soluble organic matter from atmospheric aerosol, *Talanta*, 55, 561–572, 2001.

20 Volten, H., Muñoz, O., Hovenier, J. W., de Haan, J. F., Vassen, W., van der Zande, W. J., and Waters, L. B. F. M.: WWW scattering matrix database for small mineral particles at 441.6 and 632.8 nm, *J. Quant. Spectrosc. Rad.*, 90, 191–206, 2005.

25 Wang, J., Liu, X., Christopher, S. A., Reid, J. S., Reid, E., and Maring, H.: The effect of non-sphericity on geostationary satellite retrievals of dust particles, *Geophys. Res. Lett.*, 30(24), 2293, doi:10.1029/2003GL018697, 2003.

Warren, A., Todd, M. C., Bristow, C., Chappell, A., Engelstaedter, S., M'Bainayell, S., Martins, V., and Washington, R.: The Bodele depression, Chad: Observations from the dustiest place on earth, *Geomorphology*, 92, 25–37, doi:10.1016/j.geomorph.2007.02.007, 2007.

30 Weingartner, E., Burtscher, H., and Baltensperger, H.: Hygroscopic properties of carbon and diesel soot particles, *Atmos. Environ.*, 31, 2311–2327, 1997.

World Meteorological Organization: A preliminary cloudless standard atmosphere for radiation computation, WCP-112 (World Climate Research Program, CAS, Radiation Commission of IAMAP, Boulder, Colo.), 1986.

## Effects of particle shape, hematite content and semi-external mixing

S. K. Mishra et al.

Title Page

Abstract

Introduction

Conclusions

References

Tables

Figures

⏪

⏩

◀

▶

Back

Close

Full Screen / Esc

Printer-friendly Version

Interactive Discussion

Xuana, J., Sokolik, I. N., Hao, J., Guo, F., Mao, H., and Yang, G.: Identification and characterization of sources of atmospheric mineral dust in East Asia, *Atmos. Environ.*, 38, 6239–6252, 2004.

Yang, M., Howell, S. G., Zhuang, J., and Huebert, B. J.: Attribution of aerosol light absorption to black carbon, brown carbon, and dust in China - interpretations of atmospheric measurements during EAST-AIRE, *Atmos. Chem. Phys.*, 9, 2035–2050, doi:10.5194/acp-9-2035-2009, 2009.

Zender, C. S., Bian, H., and Newman, D.: Mineral Dust Entrainment and Deposition (DEAD) model: Description and 1990s dust climatology, *J. Geophys. Res.*, 108, 4416, doi:10.1029/2002JD002775, 2003.

Zhang, H., Wang, Z. L., Guo, P. W., and Wang, Z. Z.: A modeling study of the effects of direct radiative forcing due to carbonaceous aerosol on the climate in East Asia, *Adv. Atmos. Sci.*, 26(1), 57–66, doi:10.1007/s00376-009-0057-5, 2009.

Zhao, T. X.-P., Laszlo, I., Dubovik, O., Holben, B. N., Sapper, J., Tanre, D., and Pietras, C.: A study of the effect of non-spherical dust particles on the AVHRR aerosol optical thickness retrievals, *Geophys. Res. Lett.*, 30(6), 1317, doi:10.1029/2002GL016379, 2003.

Zongbo, S., Shao, L., Jones, T. P., and Lu, S.: Microscopy and mineralogy of airborne particles collected during severe dust storm episodes in Beijing, China, *J. Geophys. Res.*, 110, D01303, doi:10.1029/2004JD005073, 2005.

## Effects of particle shape, hematite content and semi-external mixing

S. K. Mishra et al.

Title Page

Abstract

Introduction

Conclusions

References

Tables

Figures

⏪

⏩

◀

▶

Back

Close

Full Screen / Esc

Printer-friendly Version

Interactive Discussion



**Table 1.** Optical constants (at  $\lambda = 0.55 \mu\text{m}$ ) of mineral dust component for varying hematite percentage obtained from Mishra and Tripathi (2008).

Composite particle component	Hematite (%)	$N$	$K$
Mineral dust	0	1.510	0.0001
	2	1.540	0.0039
	4	1.570	0.0080
	6	1.600	0.0125
	8	1.630	0.0174

## Effects of particle shape, hematite content and semi-external mixing

S. K. Mishra et al.

Title Page

Abstract

Introduction

Conclusions

References

Tables

Figures

⏪

⏩

◀

▶

Back

Close

Full Screen / Esc

Printer-friendly Version

Interactive Discussion









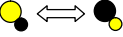






**Table 2.** Optical constants of carbonaceous components and fly-ash.

Composite particle component	Reference	$N$	$K$	$\lambda(\mu\text{m})$
Organic carbon, OC	Dinar et al. (2008)	1.595	0.0490	0.532
Brown carbon, BrC	Alexander et al. (2008)	1.670	0.2700	0.550
Black carbon, BC	Hess et al. (1998)	1.750	0.4400	0.550
Fly-ash	Liu and Swithenbank (1996)	1.500	0.0000	0.550

## Effects of particle shape, hematite content and semi-external mixing

S. K. Mishra et al.

Mineral dust mixed with the carbonaceous component	Two-sphere system	Two-spheroid system	Three-sphere system
Organic Carbon, OC 			
Brown Carbon, BrC 			
Black Carbon, BC 			

 Mineral dust (with Hematite variation 0-8%)     Fly-ash

**Fig. 1.** The pure mineral dust (shown with yellow sphere) mixed with the carbonaceous components like Organic carbon, OC, Brown carbon, BrC, and Black carbon, BC shown with pink, dark tan, and black spheres respectively (First column, top to bottom). Semi-externally mixed polluted mineral dust two-sphere and two spheroid model shapes comprising of mineral dust with OC, BrC and BC respectively (Second and third column, top to bottom). BrC mineral dust two spheroid model shape has not been modeled as BrC occurs in spherical form. The three sphere model shape of mineral dust with OC, BrC and BC respectively (Fourth column, top to bottom). Some of the three sphere systems were modeled with fly-ash (shown with grey sphere) based on the experimental observations.

Title Page

Abstract

Introduction

Conclusions

References

Tables

Figures

⏪

⏩

◀

▶

Back

Close

Full Screen / Esc

Printer-friendly Version

Interactive Discussion

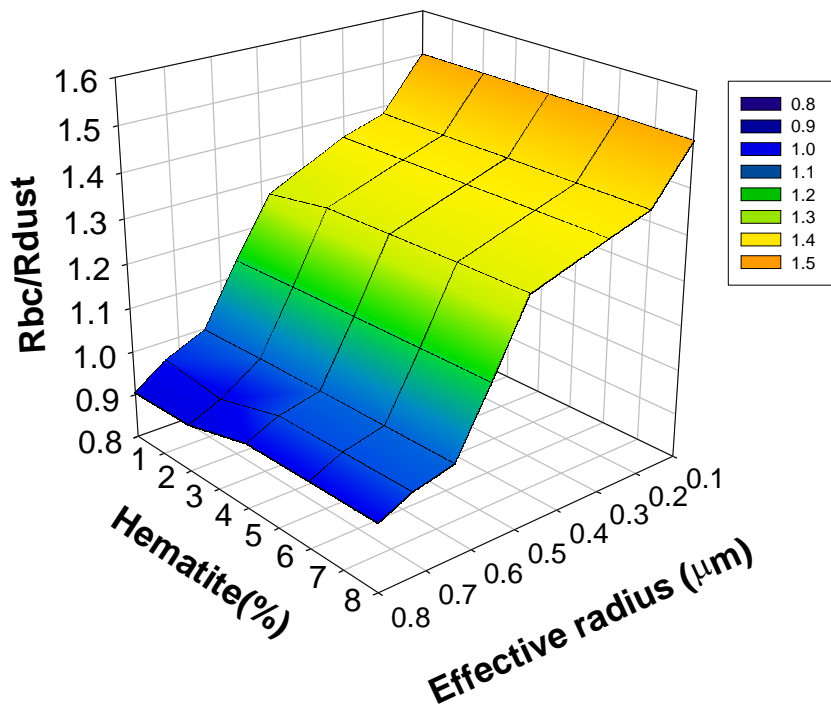


**Fig. 2.** The BC-mineral dust two sphere system with the ratio of radius of BC sphere ( $R_{BC}$ ) to that of mineral dust sphere ( $R_{dust}$ ) i.e.  $R_{BC}/R_{dust}$  for the effective volume equivalent radius of the two-sphere cluster with the varying hematite percentage in the mineral dust. Sizes of the individual particles in the cluster have been governed with the shape parameters in the DDA model. Increasing hematite causes increase in the absorption of the composite particle. Hematite variation is shown here to check the code sensitivity for the BC-mineral dust two sphere systems.

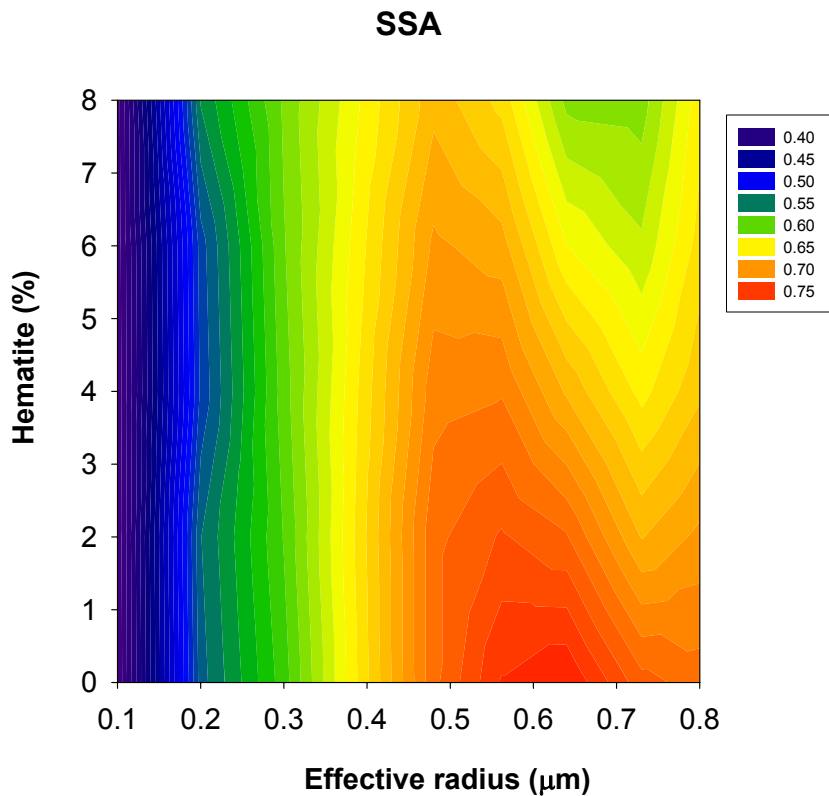


**Fig. 3.** The SSA of the BC-mineral dust two sphere system for the effective volume equivalent radius of the two-sphere cluster with the varying hematite percentage in the mineral dust.



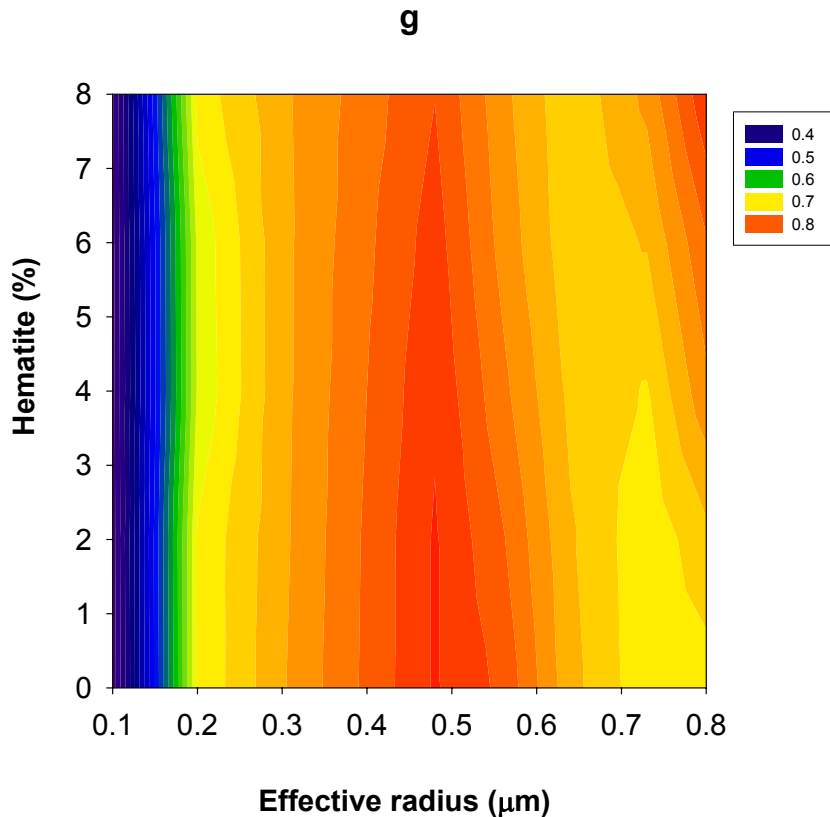


**Fig. 4.** The asymmetry parameter,  $g$  of the BC-mineral dust two sphere system for the effective volume equivalent radius of the two-sphere cluster with the varying hematite percentage in the mineral dust.

## Effects of particle shape, hematite content and semi-external mixing

S. K. Mishra et al.

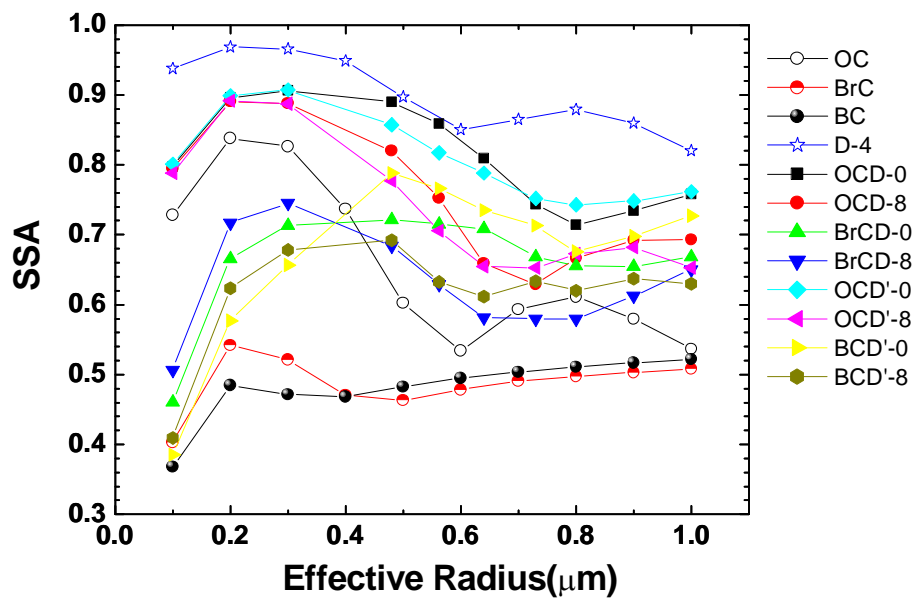


**Fig. 5.** The extinction efficiency,  $Q_{\text{ext}}$  of the BC-mineral dust two sphere system for the effective volume equivalent radius of the two-sphere cluster with the varying hematite percentage in the mineral dust.

[Title Page](#)
[Abstract](#)
[Introduction](#)
[Conclusions](#)
[References](#)
[Tables](#)
[Figures](#)
[⏪](#)
[⏩](#)
[◀](#)
[▶](#)
[Back](#)
[Close](#)
[Full Screen / Esc](#)
[Printer-friendly Version](#)
[Interactive Discussion](#)

## Effects of particle shape, hematite content and semi-external mixing

S. K. Mishra et al.

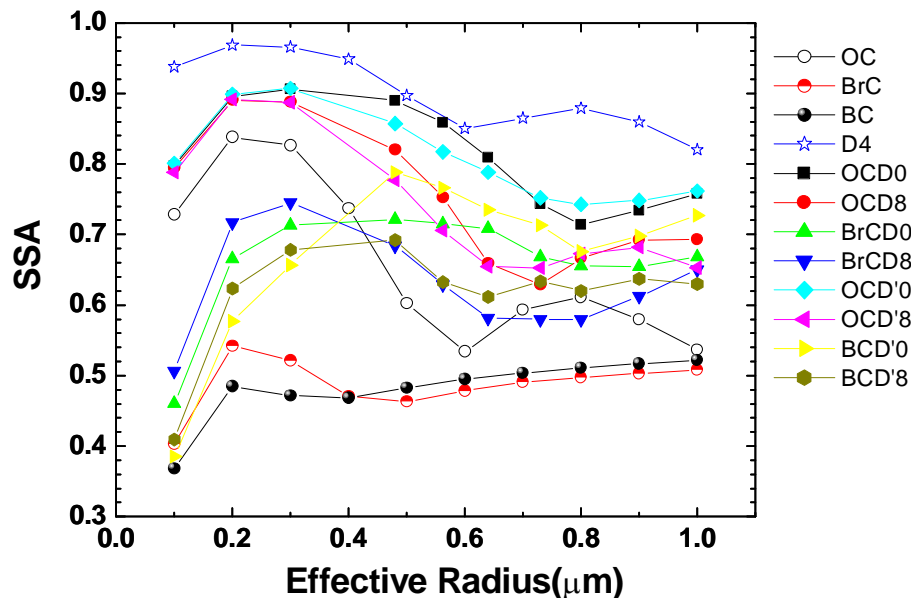


**Fig. 6.** The SSA of the 2-sphere OC-dust, BrC-dust and 2-spheroid OC-dust, BC-dust systems for the effective volume equivalent radius. The 2-sphere OC-dust and BrC-dust systems are denoted as OCD and BrCD respectively while the two spheroid systems OC-dust and BC-dust are denoted as OCD' and BCD' respectively. Each above mentioned nomenclature is followed by the hematite percentage. The 3-sphere systems are compared to that of homogeneous spheres of organic carbon (OC), brown carbon (BrC), black carbon (BC) and dust with 4% hematite (D-4).

[Title Page](#)
[Abstract](#)
[Introduction](#)
[Conclusions](#)
[References](#)
[Tables](#)
[Figures](#)
[◀](#)
[▶](#)
[◀](#)
[▶](#)
[Back](#)
[Close](#)
[Full Screen / Esc](#)
[Printer-friendly Version](#)
[Interactive Discussion](#)

## Effects of particle shape, hematite content and semi-external mixing

S. K. Mishra et al.

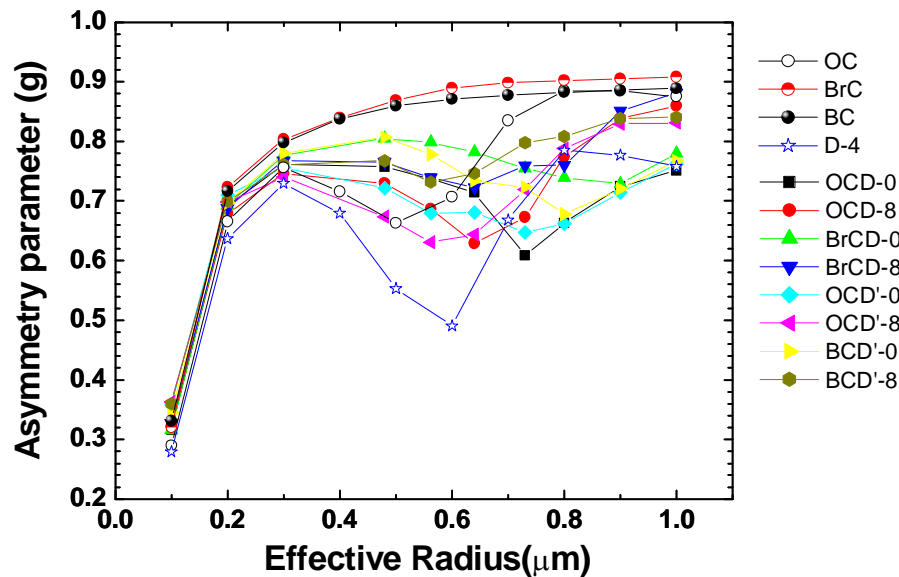


Fig. 7. The Asymmetry parameter,  $g$  for all the particle systems discussed in Fig. 6.

Title Page

Abstract

Introduction

Conclusions

References

Tables

Figures

◀

▶

◀

▶

Back

Close

Full Screen / Esc

Printer-friendly Version

Interactive Discussion

## Effects of particle shape, hematite content and semi-external mixing

S. K. Mishra et al.

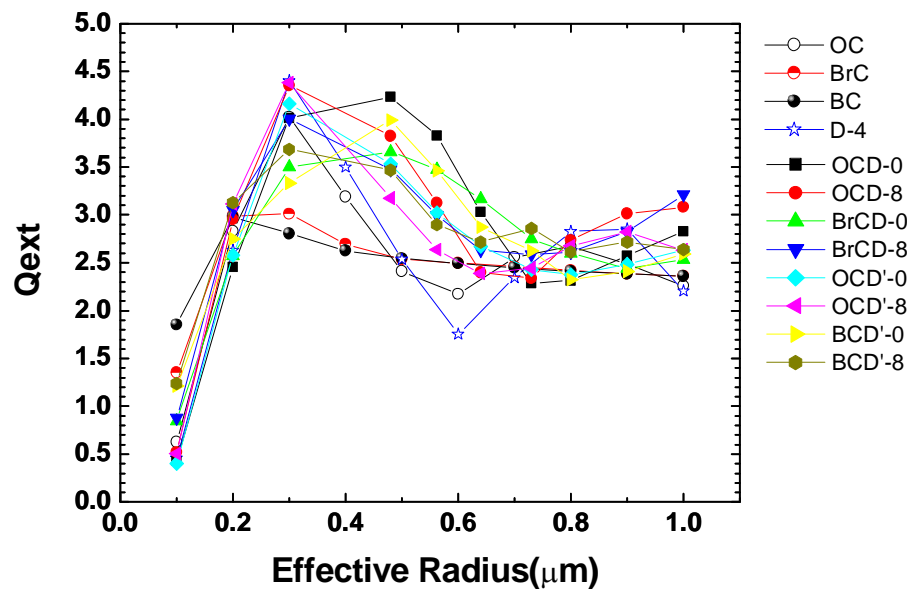


**Fig. 8.** The Extinction efficiency,  $Q_{ext}$  for all the particle systems discussed in Fig. 6.

Title Page

Abstract

Introduction

Conclusions

References

Tables

Figures

◀

▶

◀

▶

Back

Close

Full Screen / Esc

Printer-friendly Version

Interactive Discussion

## Effects of particle shape, hematite content and semi-external mixing

S. K. Mishra et al.

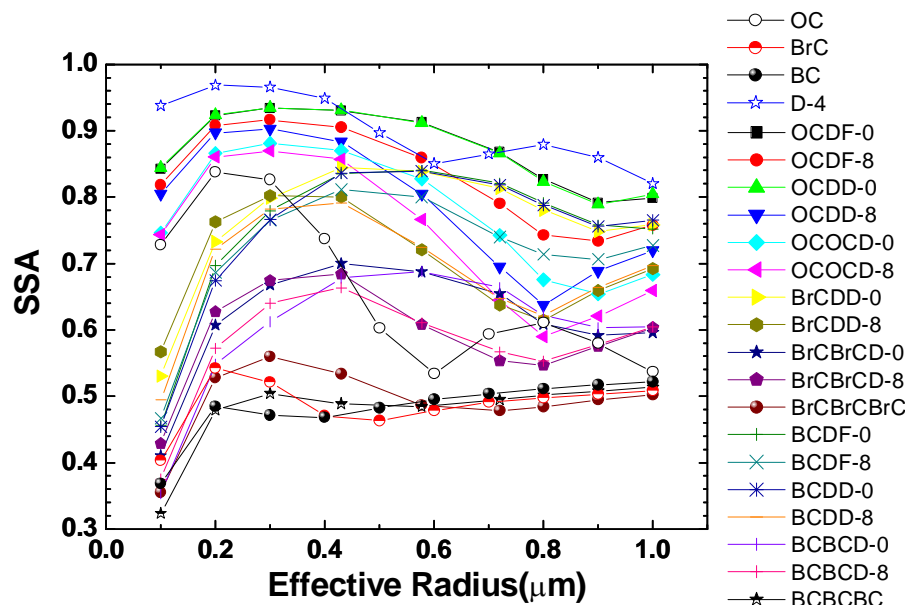


**Fig. 9.** The SSA of the 3-sphere OC-dust-flyash, OC-dust, BrC-dust, 3-sphere BrC, BC-dust-flyash, BC-dust and 3-sphere BC systems for the effective volume equivalent radius. The OC-dust-flyash and OC-dust systems are denoted as OCDF, OCDD and OCOCD respectively. The BrC-dust and BrC 3-sphere systems are denoted as BrCBrCD, BrCDD and BrCBrCBrC respectively. The BC-dust-flyash, BC-dust and BC 3-sphere systems are denoted as BCDF, BCDD, BCBCD and BCBCBC respectively. Each above mentioned nomenclature is followed by the hematite percentage. The 3-sphere systems are compared to that of homogeneous spheres of organic carbon (OC), brown carbon (BrC), black carbon (BC) and dust with 4% hematite (D-4).

Title Page

Abstract

Introduction

Conclusions

References

Tables

Figures

◀

▶

◀

▶

Back

Close

Full Screen / Esc

Printer-friendly Version

Interactive Discussion

## Effects of particle shape, hematite content and semi-external mixing

S. K. Mishra et al.

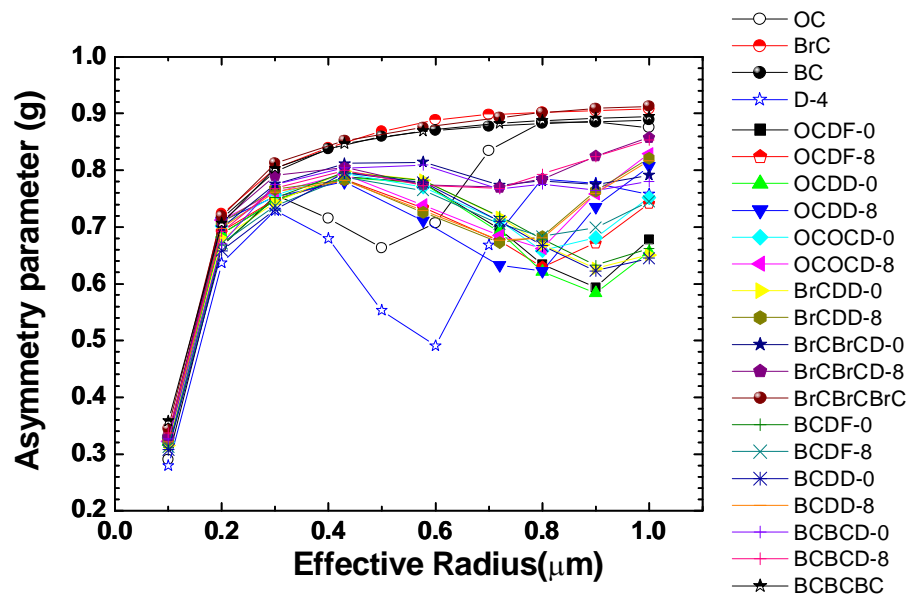


Fig. 10. The Asymmetry parameter,  $g$  for all the particle systems discussed in Fig. 9.

Title Page

Abstract

Introduction

Conclusions

References

Tables

Figures

◀

▶

◀

▶

Back

Close

Full Screen / Esc

Printer-friendly Version

Interactive Discussion

## Effects of particle shape, hematite content and semi-external mixing

S. K. Mishra et al.

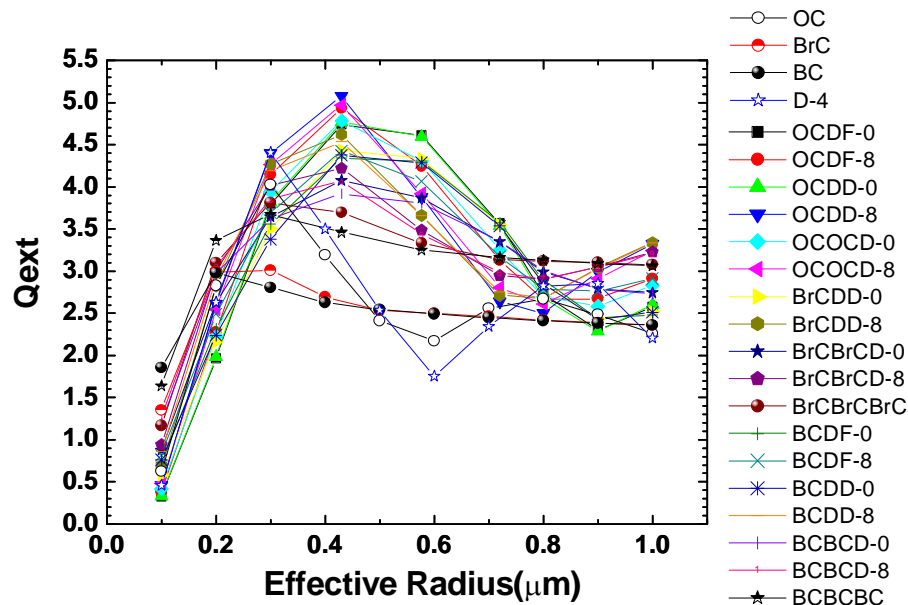


Fig. 11. The Extinction efficiency,  $Q_{\text{ext}}$  for all the particle systems discussed in Fig. 9.

Title Page

Abstract

Introduction

Conclusions

References

Tables

Figures

◀

▶

◀

▶

Back

Close

Full Screen / Esc

Printer-friendly Version

Interactive Discussion